



→ 6th ESA ADVANCED TRAINING COURSE ON LAND REMOTE SENSING

Advanced Optical

Gastellu-Etchegorry Jean-Philippe

CESBIO

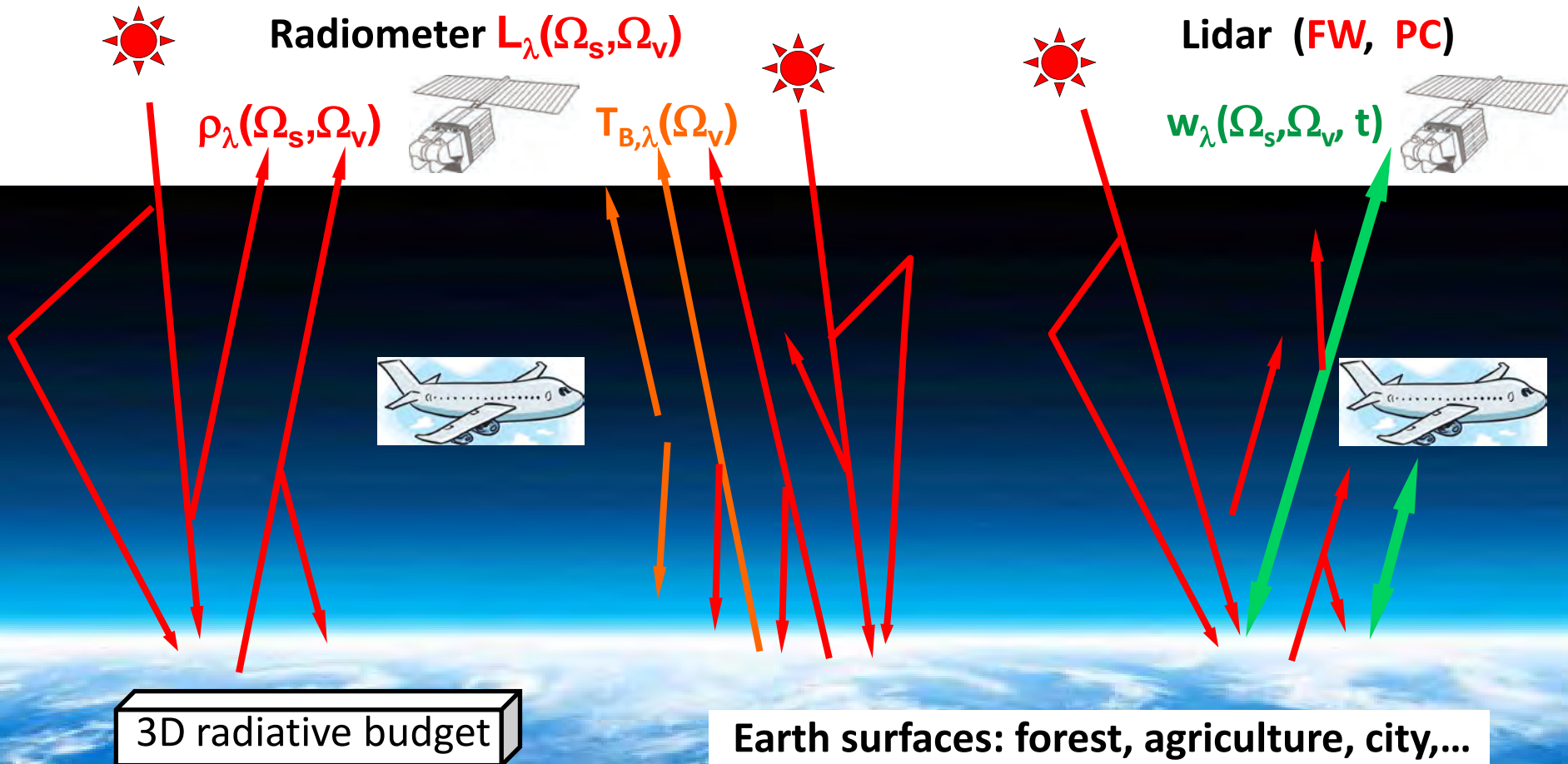
Paul Sabatier University, CNES, CNRS, IRD, France

14–18 September 2015 | University of Agronomic Science and Veterinary Medicine Bucharest | Bucharest, Romania

- Major remote sensing configurations
- Reflectance configuration: - Radiometric variables & Components of TOA radiance
- Hot spot, penumbra, 2D display of reflectance, albedo
- Thermal emission: Radiometric quantities and TOA radiance components
- The atmosphere: TOA radiance (UV → TIR)
- Modelling remote sensing signals
- Interpretation of VIS/IR and TIR satellite images
- Angular anisotropy of remote sensing signals
- Satellite / airborne sensors with finite FOV
- LiDAR

Objective: to explain remote sensing signals with physics, and remote sensing models

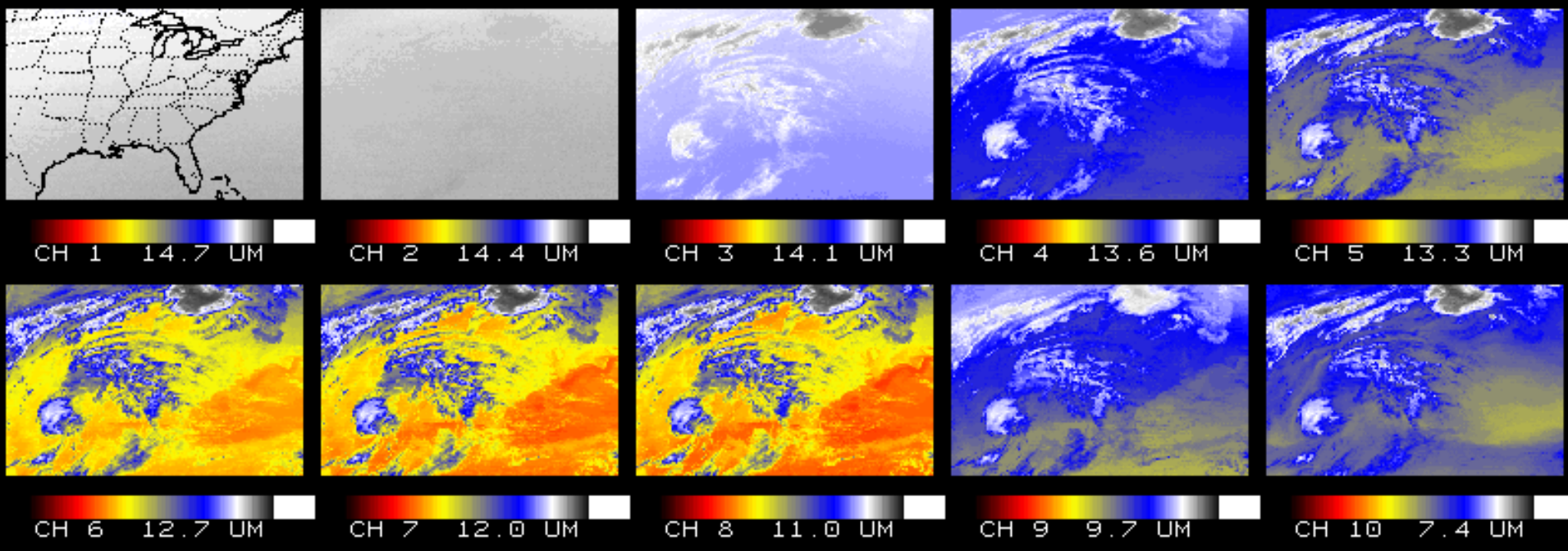
Remote sensing ($\lambda \in [0.25\mu\text{m} \ 100\mu\text{m}]$)



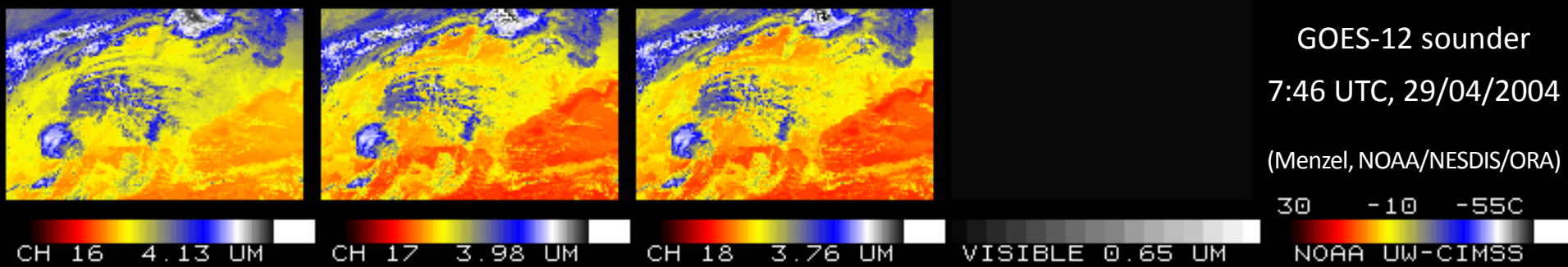
Information about Earth surfaces in remote sensing signals:

- **Spectral signature**: signal variation with wavelength \Leftrightarrow spectrometers
- **Angular signature**: signal variation with view (sun) direction \Leftrightarrow multi-view sensor,...
- **Spatial signature**: signal variation with space \Leftrightarrow high / mid spatial resolution
- **Temporal signature**: signal variation with time \Leftrightarrow sensor acquisition repetitivity
- **Architecture** / distance signature: backscattering of LiDAR pulse
- **Fluorescence** emission (specific spectral bands), **polarization**, etc.

Perception vs. spectral domain: GOES12 Sounder \Rightarrow Brightness temperature at several altitudes



- Signal is null in the visible band (0.65 μ m). Why?
- In thermal infrared (TIR) bands:
 - The low (-50C) and large (20C) signals (brightness temperature T_B) correspond to?
 - The atmosphere thermal emission changes with spectral band (*i.e.*, lower/higher T_B). Why?

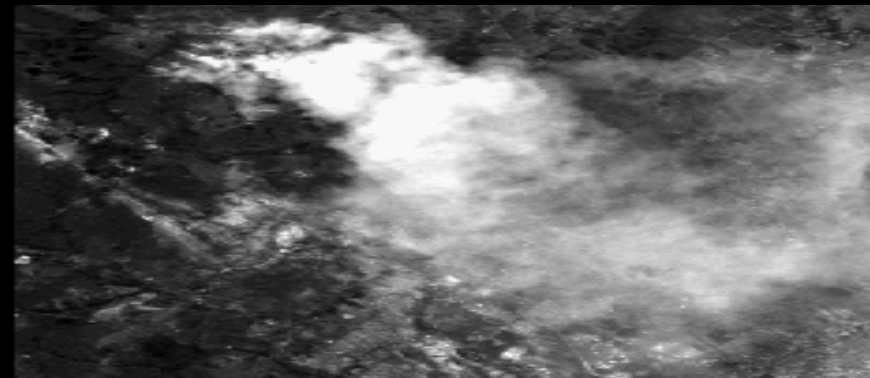


GOES-12 sounder
7:46 UTC, 29/04/2004
(Menzel, NOAA/NESDIS/ORR)

Perception vs. spectral domain: AVIRIS images of forest clearing fire (Cuiaba - Brazil, 25/08/1995)



True color



500.5 nm



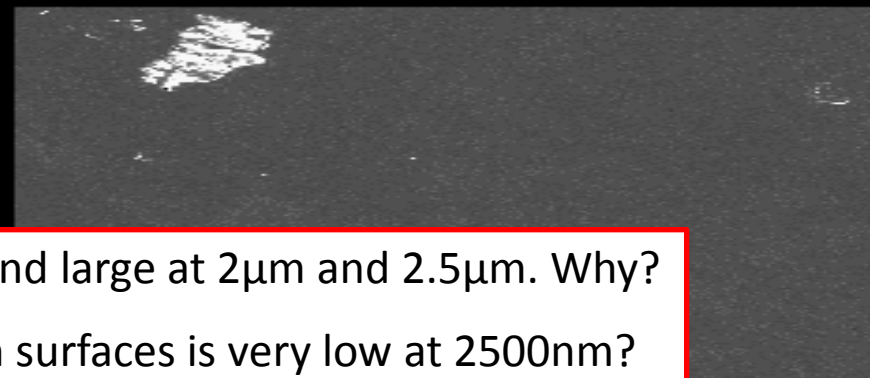
1000.2 nm



1501.4 nm



2000.5 nm



2508.5 nm

- Fire signal is low at $1\mu\text{m}$ and large at $2\mu\text{m}$ and $2.5\mu\text{m}$. Why?
- Why the signal from Earth surfaces is very low at 2500nm ?

Perception vs. spectral domain and passive vs. active sensor: G-LIHT images (NASA)

Airborne G-LIHT sensor:

Scanning lidar

Swath width/FOV	387 m (60°)
Footprint diameter	10 cm (0.3 mrad)
Range precision	5 cm (2 σ)
Sampling density at surface	6 pulses m ⁻²
Max. returns per pulse	8

Irradiance spectrometer

Swath width/FOV	hemispheric (180°)
Spectral range	350 to 1,100 nm
Sample/Band width	1.5 and 1.5 nm
Acquisition rate	1 Hz

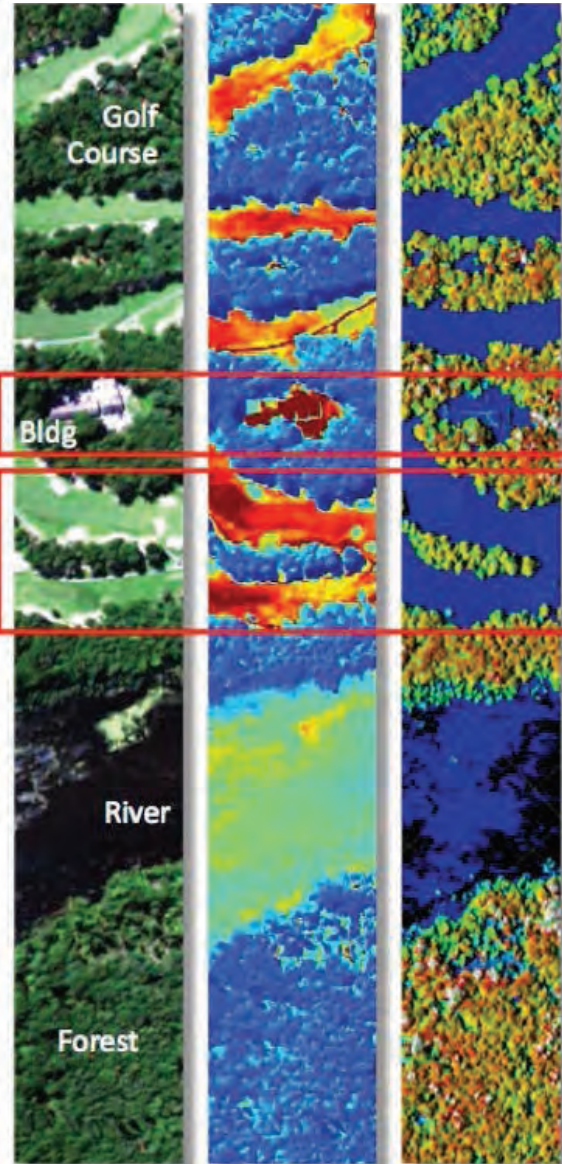
Imaging spectrometer

Swath width/FOV	310 m (50°)
Cross track pixels	1,004
Spectral range	420 to 950 nm
Sample/Band width	1.5 and 5.0 nm
Acquisition rate	50 Hz

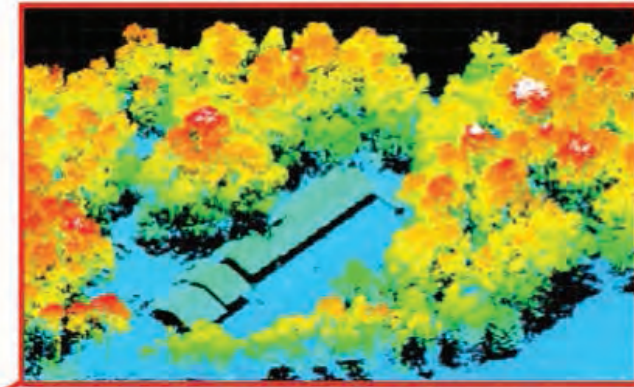
Thermal camera

Swath width/FOV	173 m (30°)
Imaging array size	384 × 288
Spectral range	8 to 14 μ m
Sensitivity (NETD)	>50 mK at 30°C
Acquisition rate	25 Hz

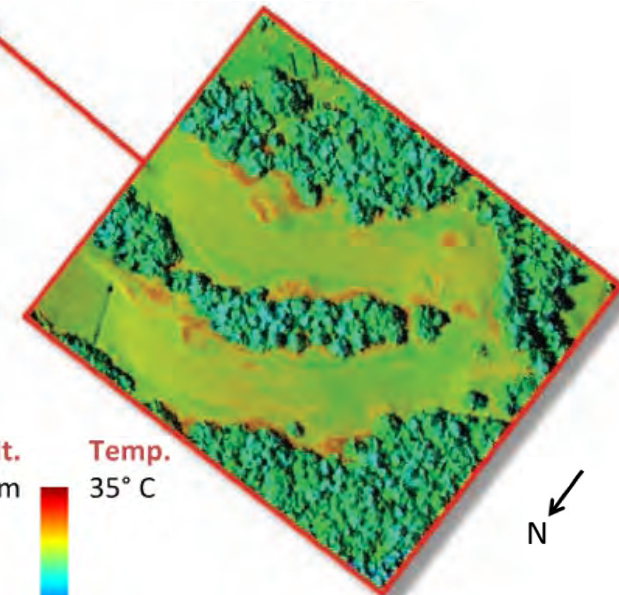
RGB color Brightness DSM \Rightarrow DEM,
composite temperature tree height,...



3D vegetation structure



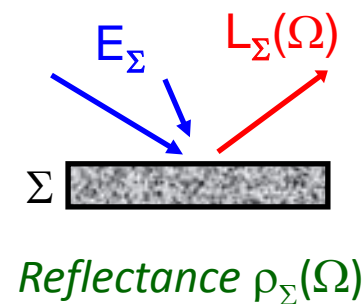
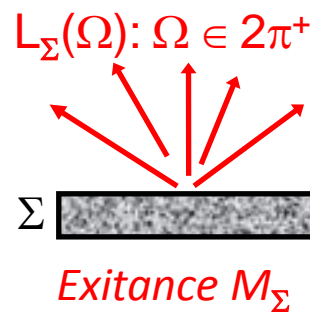
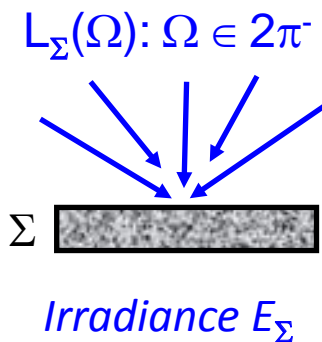
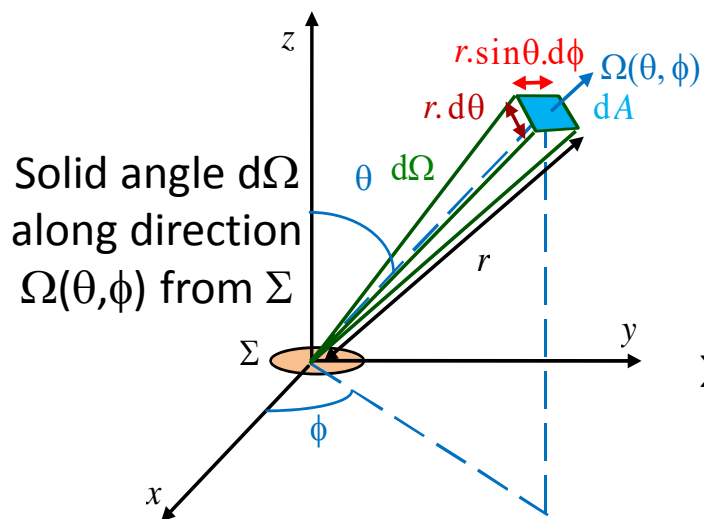
LiDAR apparent reflectance



- Why brightness temperature is larger for grass than for trees?
- How 3D vegetation is obtained?
- What is LiDAR apparent ρ ?
- What is the usefulness of the irradiance spectrometer?

Physical bases about radiation: *definitions*

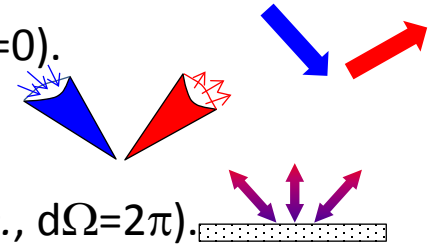
- **Solid angle** $d\Omega$ of direction $\Omega(\theta, \phi)$: $d\Omega = \sin\theta \cdot \cos\phi \cdot d\theta \cdot d\phi$ with θ = zenith and ϕ = azimuth
- **Radiance** $L_{\Sigma}(\Omega)$ of Σ along (Ω) : $L_{\Sigma, \lambda}(\Omega)$: $W/m^2/sr/\mu m$ (/ effective m^2 !), $L_{\Sigma, \Delta\lambda}(\Omega)$: $W/m^2/sr$
- **Irradiance** E_{Σ} of Σ (in flux): $E_{\Sigma, \lambda} = \int_{2\pi^-} L_{\Sigma, \lambda}(\Omega) \cdot |\cos\theta| \cdot d\Omega$ $W/m^2/\mu m$ $E_{\Sigma, \Delta\lambda} = \int_{2\pi^-} L_{\Sigma, \Delta\lambda}(\Omega) \cdot |\cos\theta| \cdot d\Omega$ W/m^2
- **Exitance** M_{Σ} of Σ (out flux): $M_{\Sigma, \lambda} = \int_{2\pi^+} L_{\Sigma, \lambda}(\Omega) \cdot \cos\theta \cdot d\Omega$ $W/m^2/\mu m$ $M_{\Sigma, \Delta\lambda} = \int_{2\pi^+} L_{\Sigma, \Delta\lambda}(\Omega) \cdot \cos\theta \cdot d\Omega$ W/m^2
- **Reflectance factor** $\rho_{\Sigma}(\Omega)$ of Σ along (Ω) : $\rho_{\Sigma, \lambda}(\Omega) = \frac{\pi \cdot L_{\Sigma, \lambda}(\Omega)}{E_{\Sigma, \lambda}}$ if Σ is lambertian: $\rho_{\Sigma, \lambda}(\Omega) = cst$



☞ What is the physical quantity that is measured by a satellite radiometer?

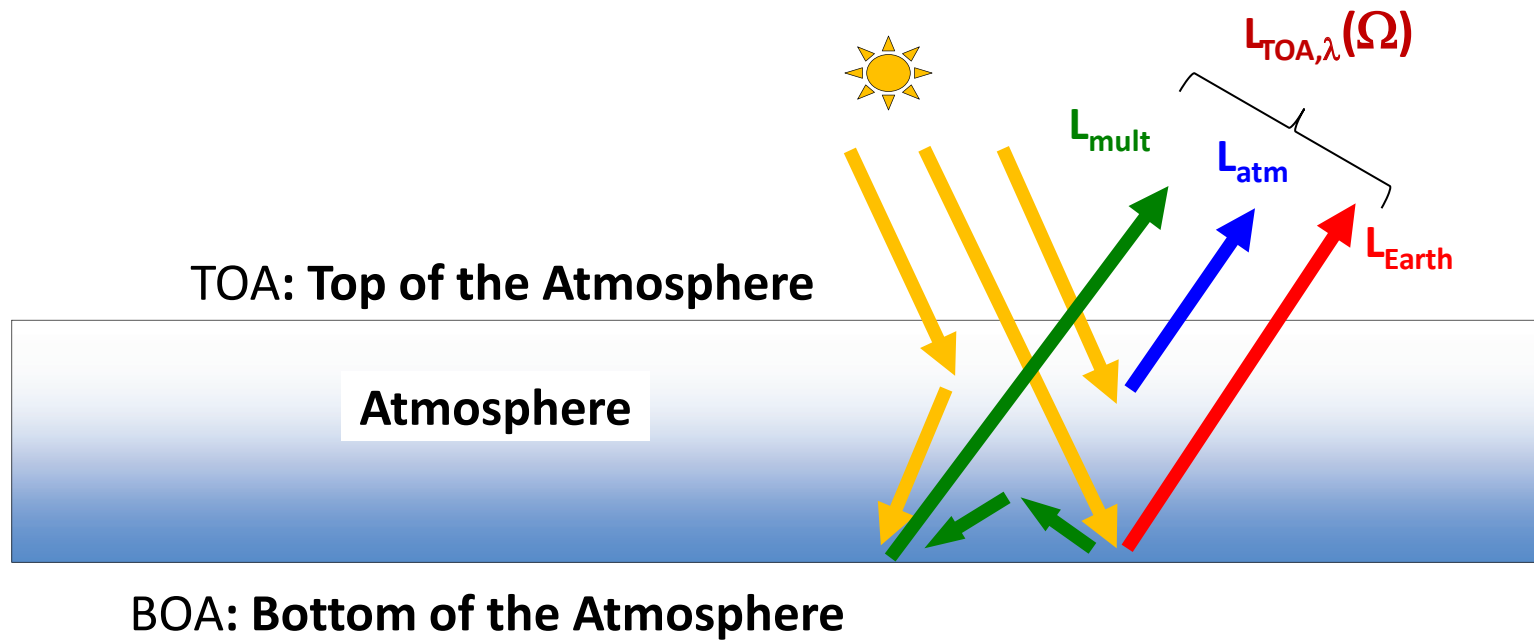
Physical bases about radiation: different reflectance factors (direct d, hemispherical h, conical c)

- **In** or **Out** 'direct' flux (index d): flux along a unique direction (*i.e.*, $d\Omega=0$).
- **In** or **Out** 'conical' flux (index c): flux within a cone (Ω , $d\Omega\neq 0$).
- **In** or **Out** 'hemispherical' flux (index h): flux within an hemisphere (*i.e.*, $d\Omega=2\pi$).



- ☞ Which reflectance is derived from the measurement of a satellite radiometer?
- ☞ Which reflectance is used for computing the albedo of our planet?

Physical bases about radiation: **Satellite signal (TOA radiance) $L_{TOA,\lambda}(\Omega)$ - short wavelengths**



$$L_{TOA,\lambda}(\Omega) = \text{"Radiance } L_{Earth,TOA,\lambda}(\Omega) \text{ due to scattering of sun flux by the Earth, only"}$$

$$+$$

$$\text{"Radiance } L_{atm,TOA,\lambda}(\Omega) \text{ due to scattering of sun flux by the Atmosphere, only"}$$

$$+$$

$$\text{"Radiance } L_{mult,TOA,\lambda}(\Omega) \text{ due to scattering of sun flux by \{Earth + Atmosphere\}"}$$

Physical bases about radiation: **Lambertian and natural surfaces**

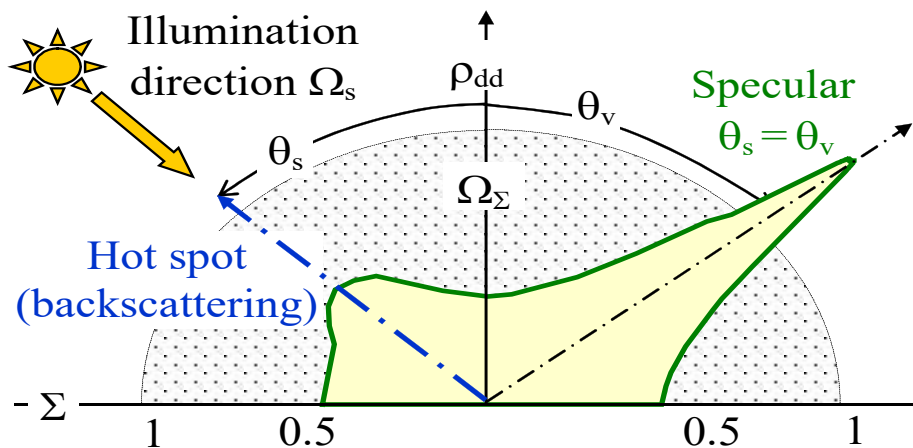
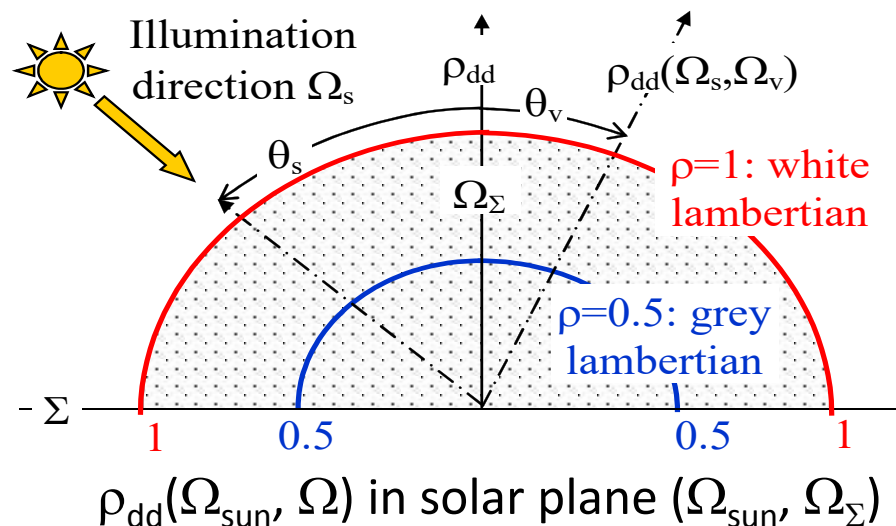
☞ How can there be hot spot? Indeed, a sensor with the sun behind it should see its own shadow...

Lambertian surface: $\rho_{dd} = \rho_{dh} = \rho_{hd} = \rho_{hh} = \text{cst.}$

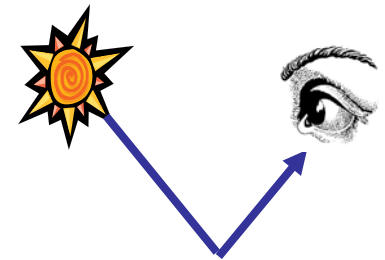
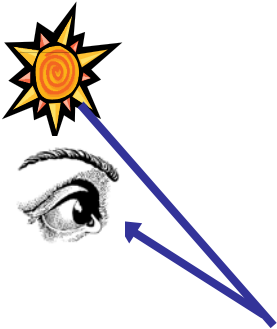
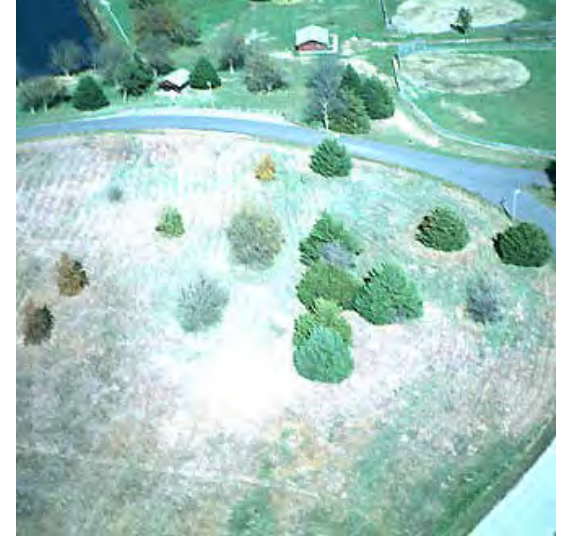
- White lambertian surface: $\rho = 1$
- Grey lambertian surface: $\rho = \text{cst} < 1$.

Natural surface: $\rho_{dd}(\Omega)$ varies with (Ω) .

Here, ρ_{dd} is maximal for specular direction (water?) with local maximum (vegetation?) for sun direction (hot spot: the sensor does not see shadow)

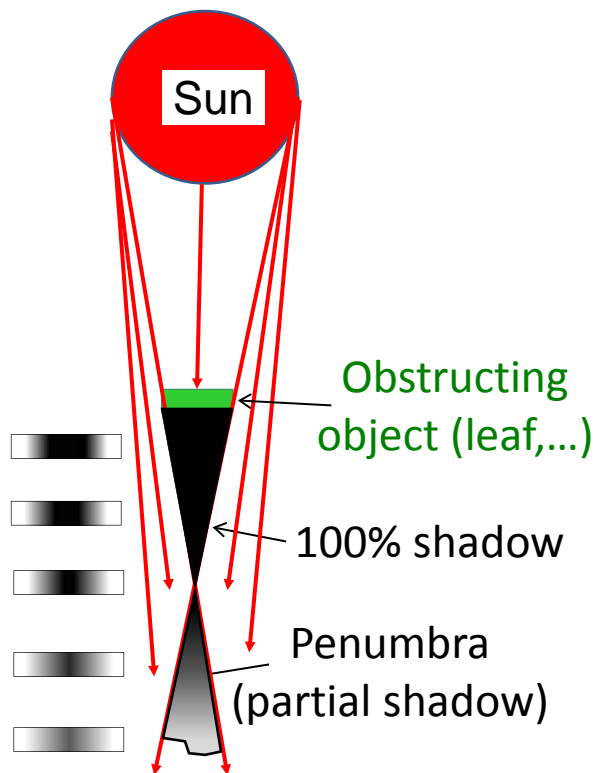


The hot spot (backscattering effect): examples



From Donald Deering

Penumbra effect



Sun rays are not parallel
⇒ shadow is total at short distance and more and more partial as distance increases

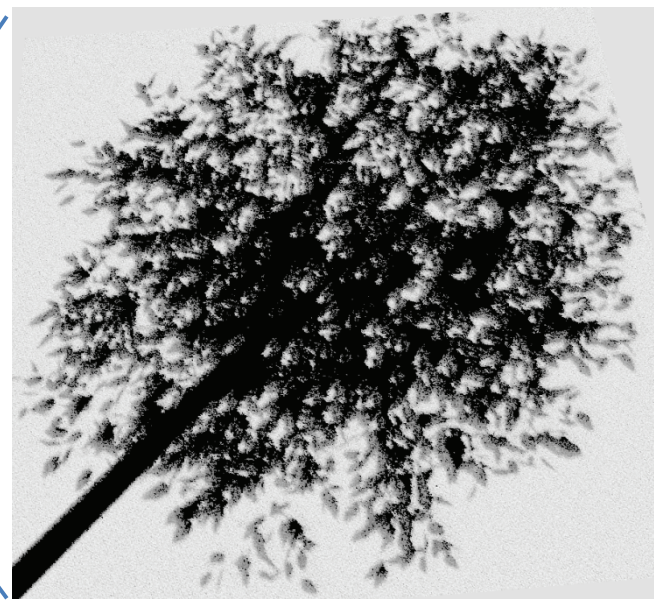
DART simulation



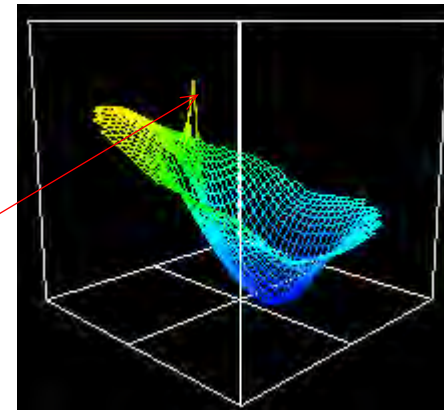
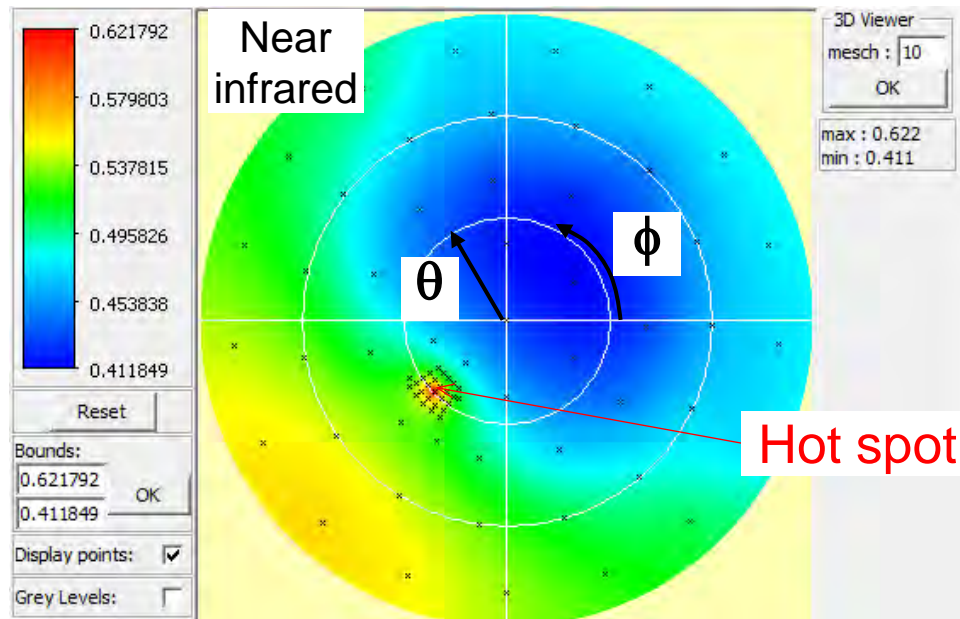
Parallel sun rays



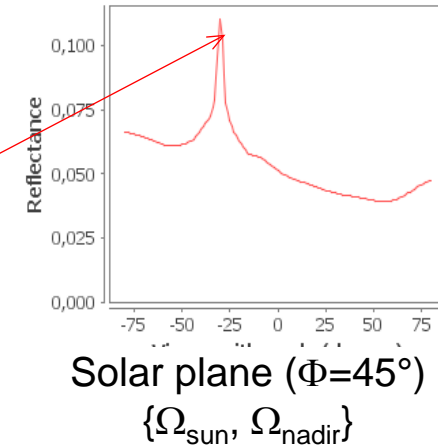
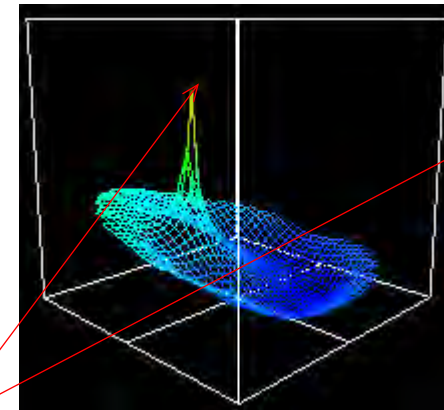
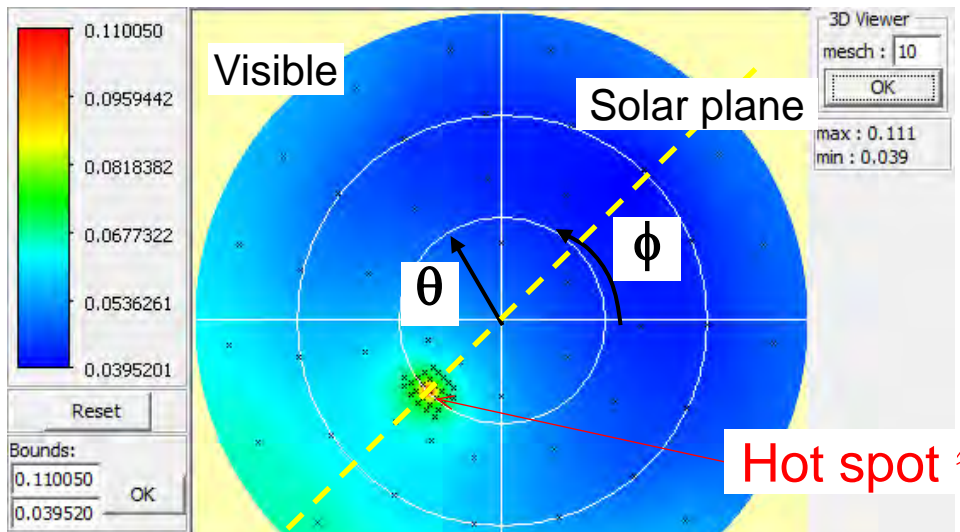
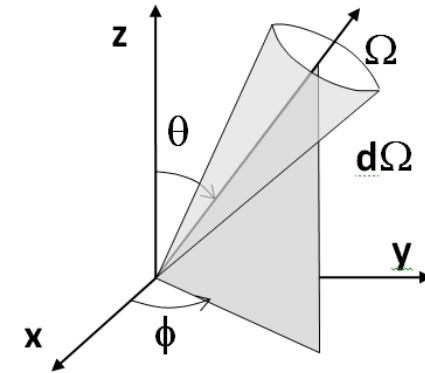
Actual sun rays: $\Delta\Omega_{\text{sun}} = 32'$



Physical bases about radiation: 1D, 2D (polar) and 3D plots of vegetation reflectance



Displays of DART model



☞ For large view zenith angles θ_{view} vegetation reflectance increases in near infrared (top) and decreases in the visible (bottom). Which simple landscape (tree + bare ground) can explain it?

Albedo and spectral reflectance of Earth surface elements

Albedo (A_{dh} or A_{hh}): integral of reflectance $\rho_\lambda(\Omega_s, \Omega_v)$ weighted by incident flux $L_\lambda(\Omega_s)$ over scattering directions ($2\pi^+$) and all / part of the spectrum.

$$A_{dh}(\Delta\Omega_s=0, \Delta\lambda) = \frac{\text{Exitance: reflexion over } 2\pi^+}{\text{Irradiance (d) along } \Omega_s} = \frac{1}{\pi} \frac{\int_{\Delta\lambda} \int_{2\pi} \rho_{dd}(\Omega_s, \Omega_v, \lambda) \cdot \mu_v \cdot E_\lambda(\Omega_s) \cdot \mu_s \cdot d\Omega_v \cdot d\lambda}{\int_{\Delta\lambda} E_\lambda(\Omega_s) \cdot \mu_s \cdot d\lambda} \quad \text{with } \Delta\lambda \approx [0.2 \text{ } 4 \text{ } \mu\text{m}]$$

At the Earth surface, one uses often: $A_{hh}(2\pi^-, \Delta\lambda) = \frac{\text{Exitance: reflexion over } 2\pi^+}{\text{Irradiance (h) along } 2\pi^-}$

Material	Albedo (%)
<i>Planet Earth</i>	≈ 33 (≈ 36 for Visible domain)
<i>Cloud (stratus)</i> : - depth < 200 m	5-65
- depth [200 1000 m]	30-85
<i>Snow</i> : fresh and dry / old	75 - 90 / 45 - 70
<i>Ground</i> : - white sand	35 - 40; increases from blue to red
- dark moist /dry	5 - 6 / 5 - 15; increases from blue to red
<i>Vegetation</i> : green crop / forest	5 - 15 / 10 ; maximum in the green
<i>Water</i> : sun zenith 0°/30°/60°/70°/80°/85°/>87°	2 / 2,2 / 6 / 13,4 / 35,8 / ≈60 / >90

Very variable albedo / reflectance values

Physical bases about radiation: **Thermal emission (Planck's law) and brightness temperature**

Planck's law: $L_{B,\lambda}(\Omega) = \frac{2 \cdot h \cdot c^2}{\lambda^5 \cdot (e^{\lambda k T} - 1)} \cdot \frac{hc}{\lambda^5}$ (W/m²/sr/m) with $h = 6.63 \cdot 10^{-34}$ J.s, $k = 1.3807 \cdot 10^{-23}$ J/K

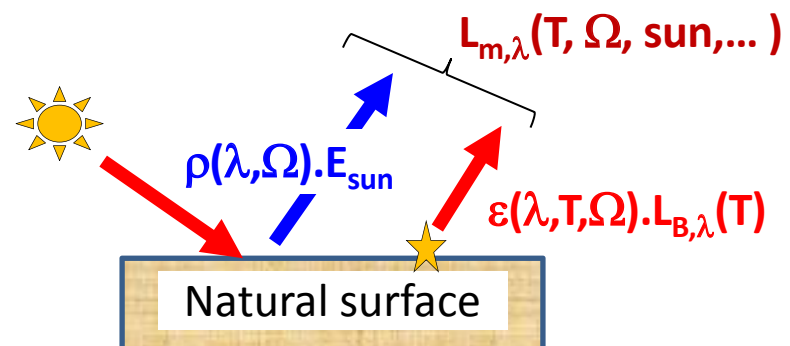
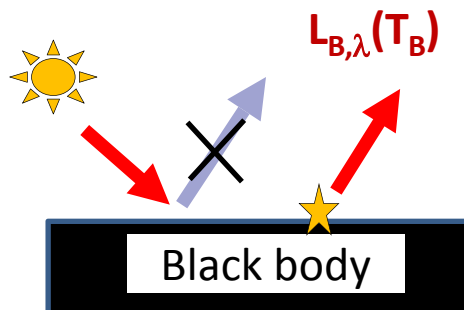
Wien law: $M(\lambda)$ is maximal for $\lambda_m = \frac{a}{T}$ (a=2899 μm.K)

Stephan-Boltzmann law: $M = \int_{\infty} L_{B,\lambda} \cdot d\lambda = \sigma \cdot T^4$, with $\sigma = 5.6704 \cdot 10^{-8}$ W/m²/K⁴

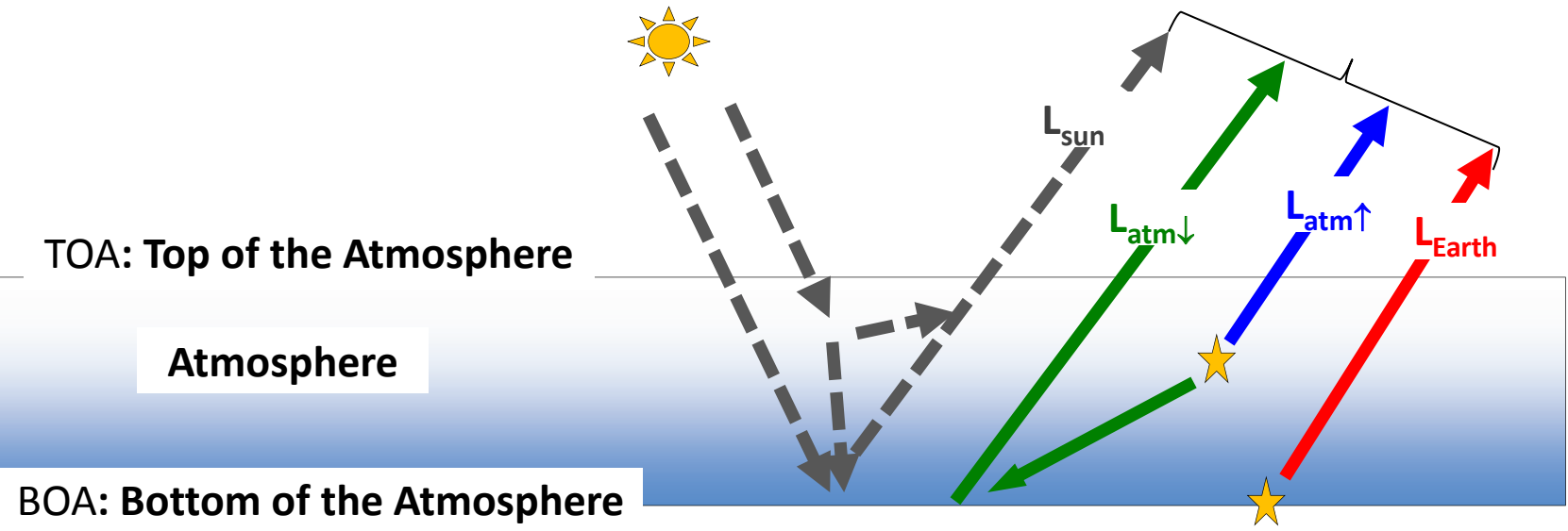
Emissivity $\epsilon(\lambda, T, \Omega)$: natural body $\Rightarrow L_{\lambda}(T, \Omega) = \epsilon(\lambda, T, \Omega) \cdot L_{B,\lambda}(T)$, with $\epsilon(\lambda, T, \Omega) = 1 - \rho_{hd}(\lambda, T, \Omega)$

Brightness temperature T_B : temperature of the blackbody that emits the measured radiance L_m

$$L_{m,\lambda}(\Omega) = L_{B,\lambda}(T_B) \Rightarrow T_B = L_{B,\lambda}^{-1}(L_{m,\lambda}(\Omega)) = f(\lambda, T, \Omega)$$



Physical bases about radiation: **Satellite signal (TOA radiance) $L_{TOA,\lambda}(\Omega)$ - long wavelengths**



$L_{TOA,\lambda}(\Omega)$ = "Radiance $L_{Earth,TOA,\lambda}(\Omega)$ due to thermal emission by the Earth, only"

+

"Radiance $L_{atm\uparrow,TOA,\lambda}(\Omega)$ due to thermal emission by the Atmosphere, only"

+

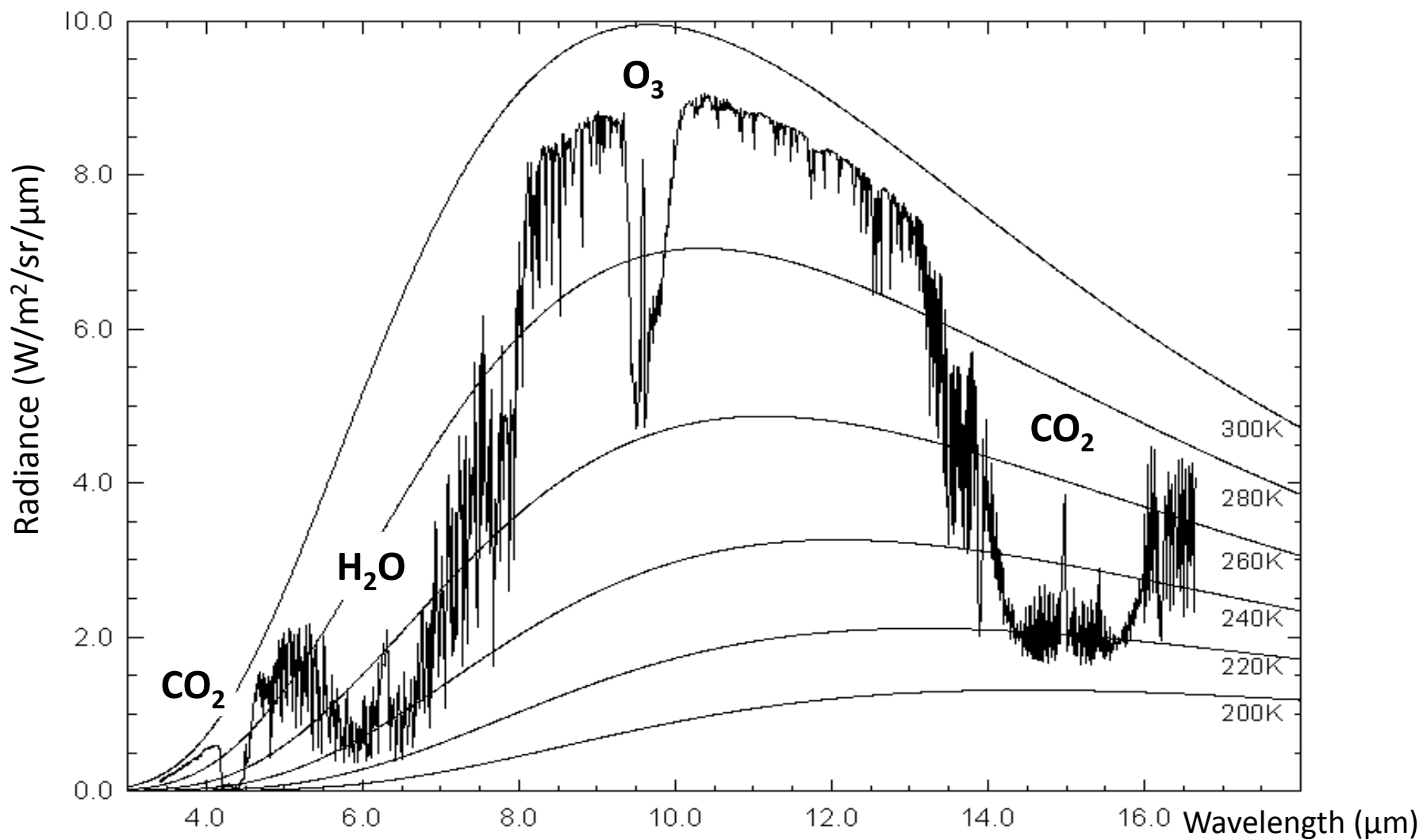
"Radiance $L_{atm\downarrow,TOA,\lambda}(\Omega)$ due to Earth scattering of Atmosphere thermal emission"

+

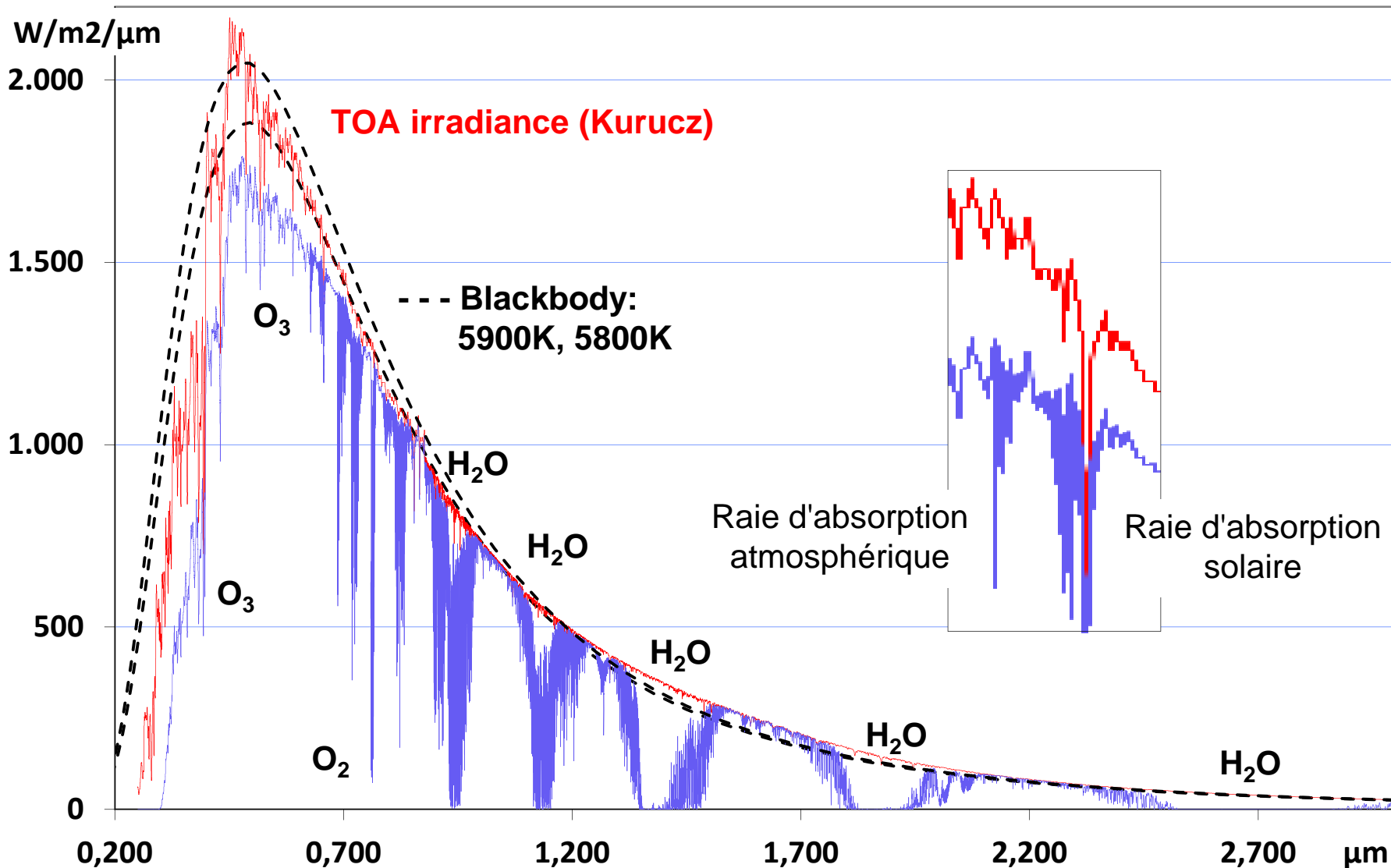
"Radiance $L_{sun,TOA,\lambda}(\Omega)$ due to {Earth, Atmosphere} scattering of sun radiation"

($L_{sun,TOA,\lambda}(\Omega) = 0$ at night, and usually neglected for $\lambda > 4\mu m$)

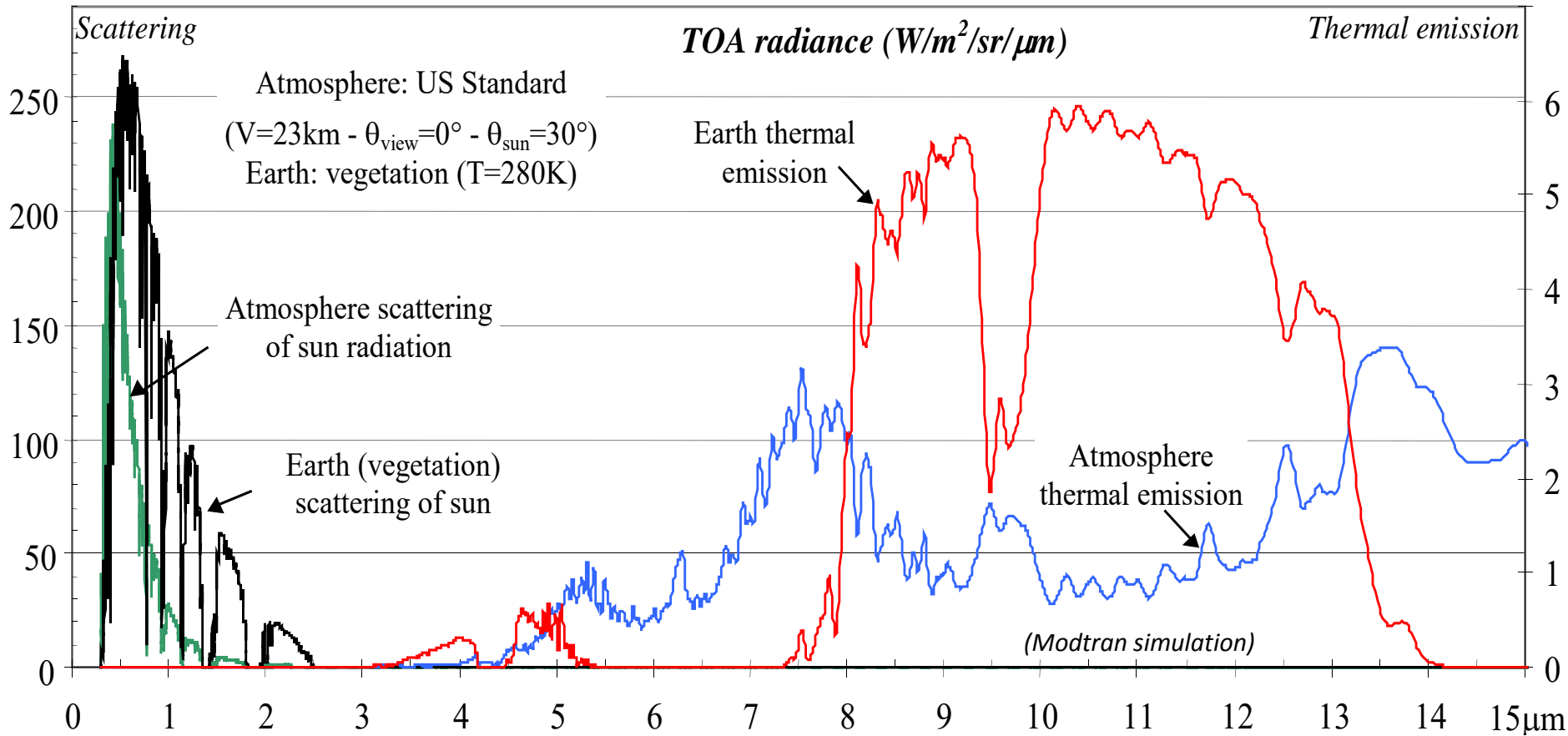
Physical bases about radiation: **TOA radiance vs. Blackbody radiance (Planck's law)**



TOA and BOA sun spectral irradiance

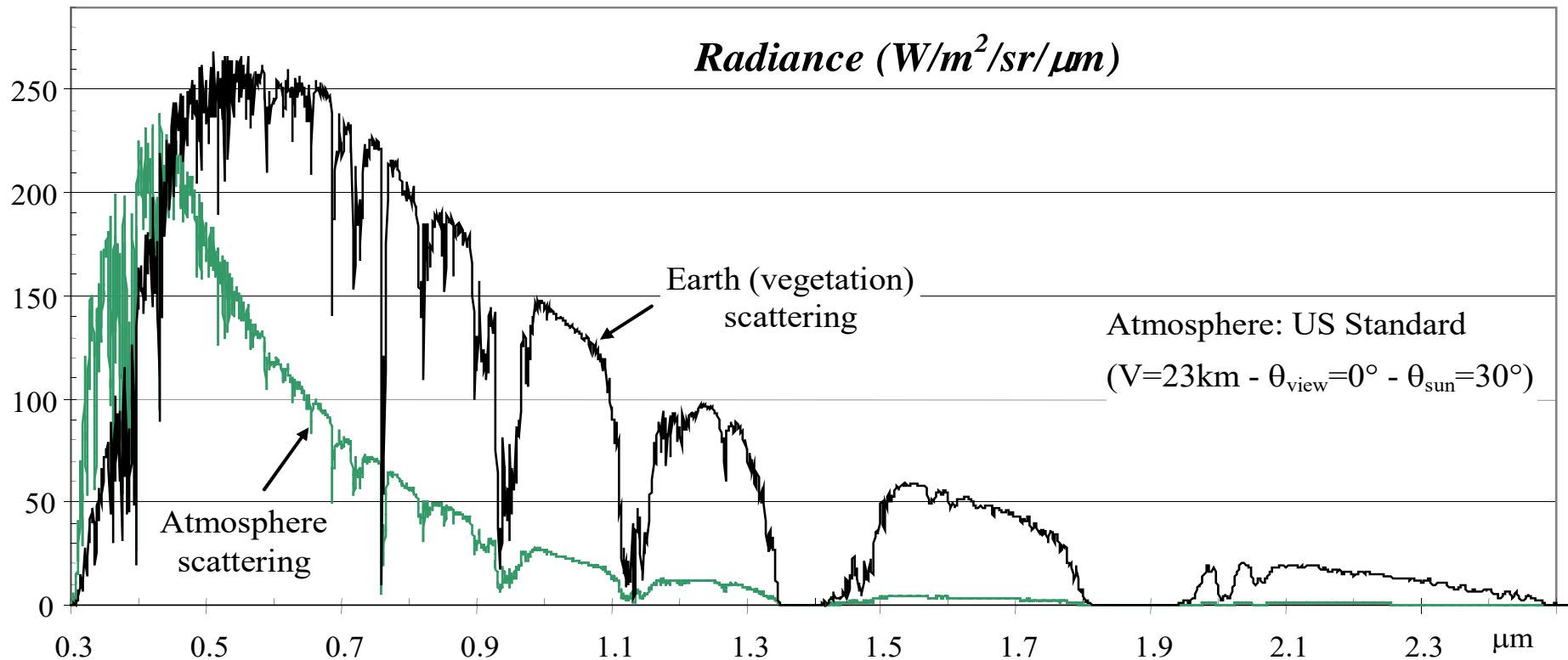


TOA radiance components: Earth and atmosphere scattering / thermal emission



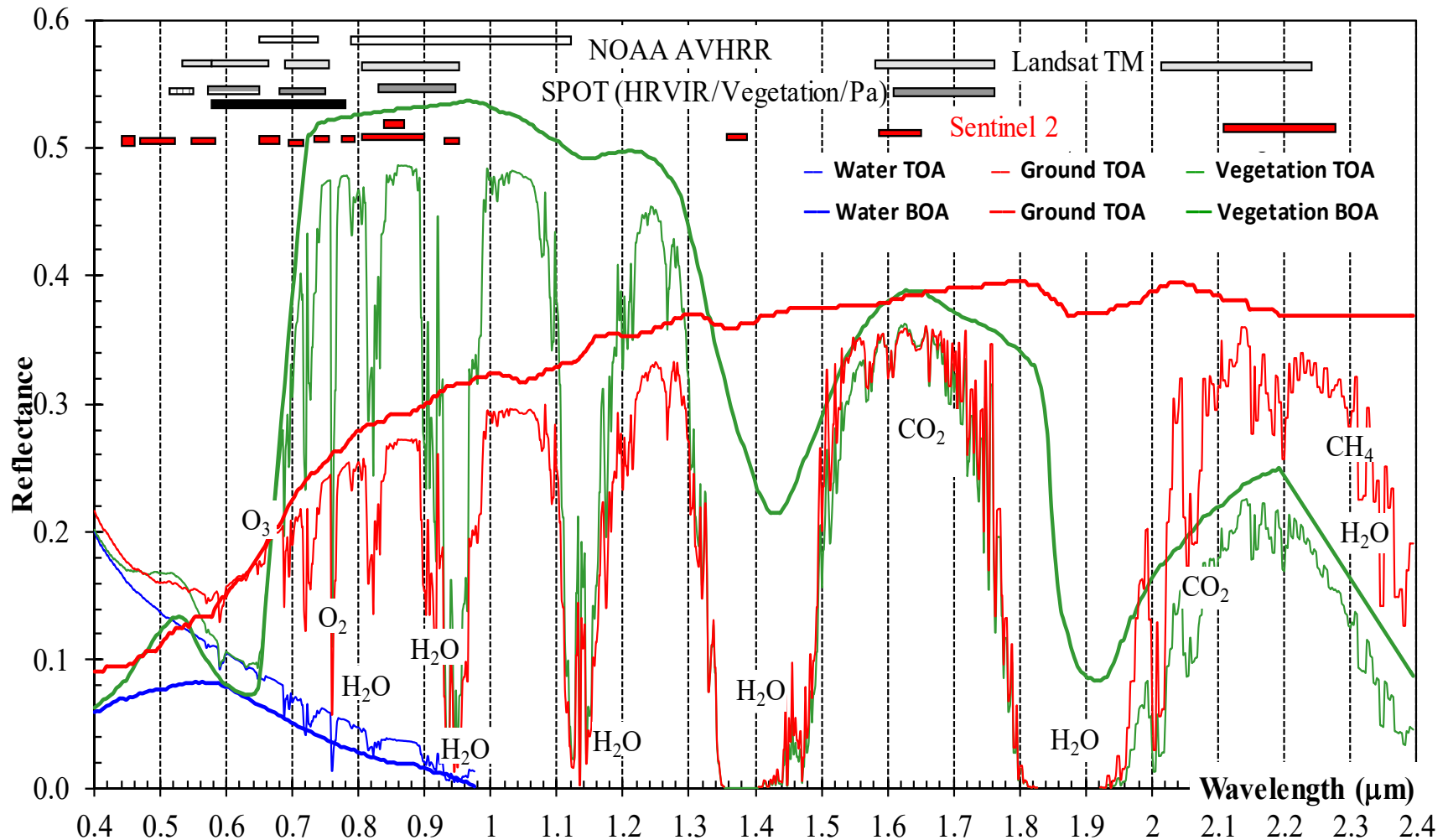
☞ For which wavelengths can we consider that TOA radiance is mostly due to either Earth surface scattering or thermal emission?

TOA radiance components: Earth and atmosphere scattering



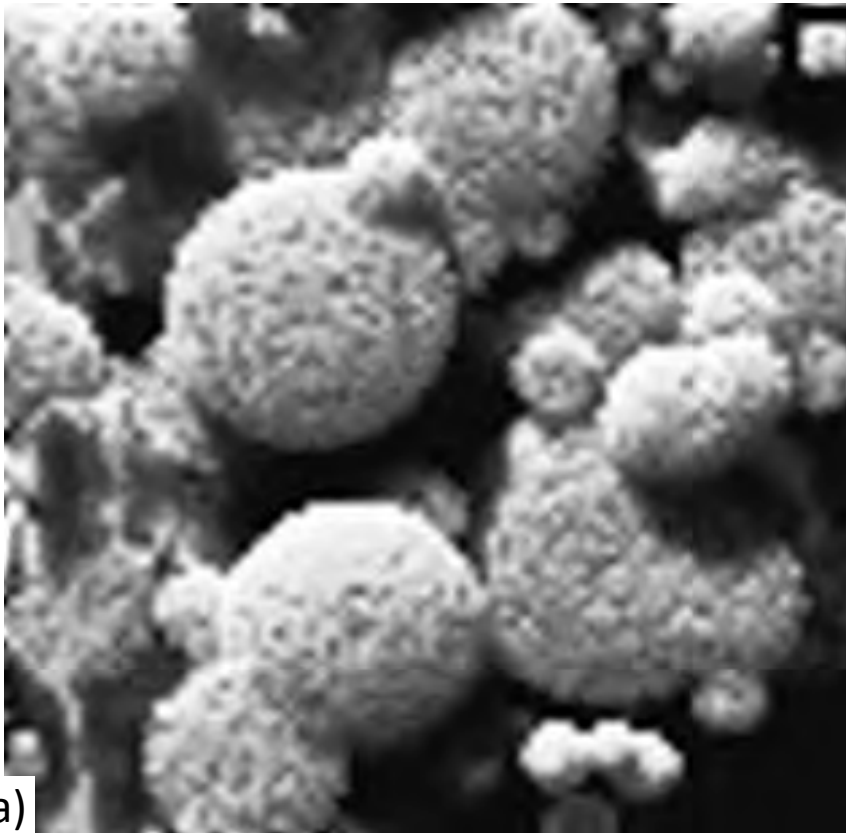
👉 How does the relative influence of atmosphere change with (θ_v , θ_s , V , etc.)?

BOA and TOA spectra of water, ground and vegetation

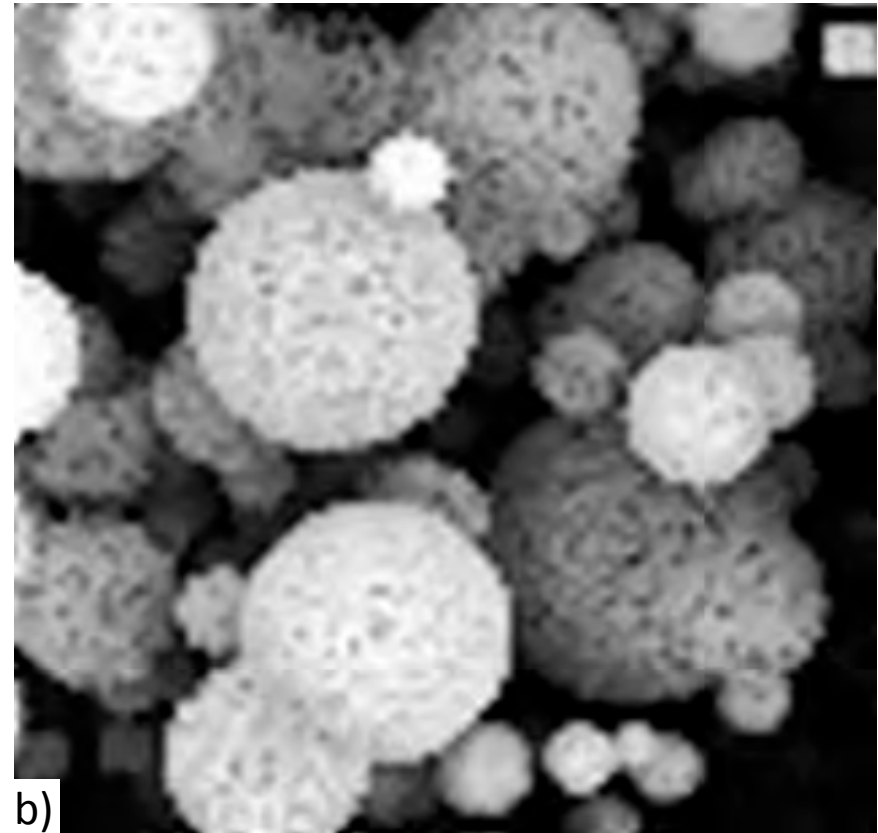


- ☞ For all surfaces, with $\lambda < 0.55\mu\text{m}$, TOA reflectance is larger than BOA reflectance. Why?
- ☞ For ground, TOA reflectance is larger than BOA reflectance for $\lambda < 0.55\mu\text{m}$, and smaller for $\lambda > 0.65\mu\text{m}$, whereas TOA water reflectance is always larger than BOA water reflectance. Why?

Sky illumination: nadir image of a tropical forest (Sumatra, Indonesia) with 2 sky illuminations



a)

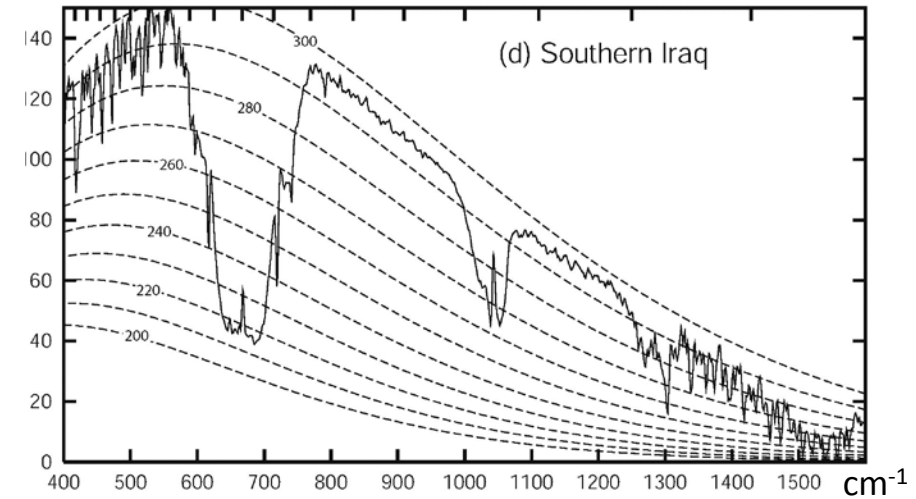
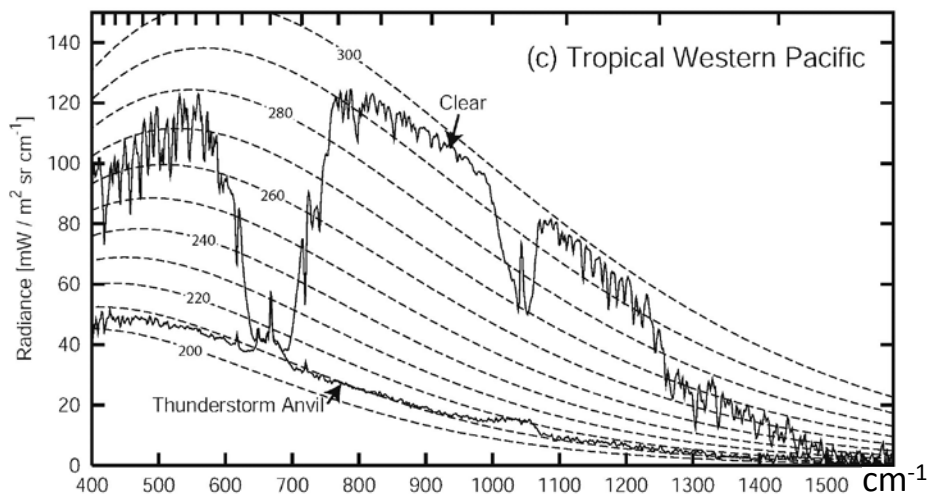
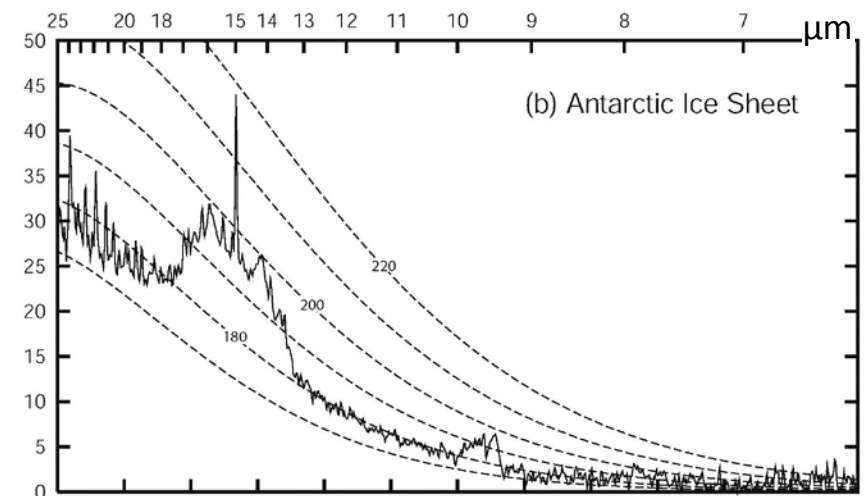
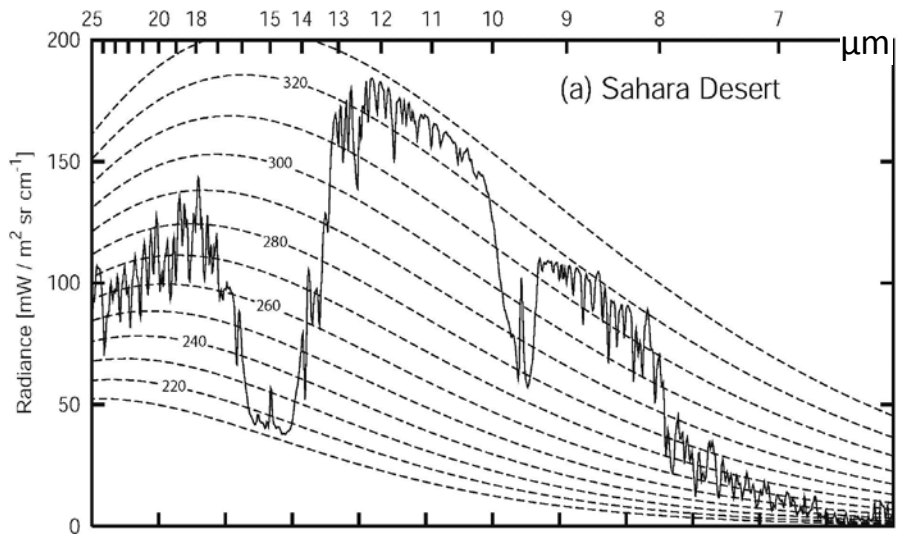


b)

a) $SKYL = 0$, $\theta_s = 35^\circ$. b) $SKYL = 1$. $SKYL = \frac{\text{Atmosphere irradiance}}{\text{Total irradiance}}$. Simulations with DART model.

☞ Does a SKYL increase, makes the reflectance of Earth surfaces larger, more anisotropic?

TIR satellite spectra: Nimbus 4 Iris (Petty G., 2006; www.sundogpublishing.com/AtmosRad/index.html)



Atmosphere absorption bands: CO_2 : $\approx 15\mu\text{m}$, O_3 : $\approx 9.5\mu\text{m}$, H_2O : $\approx 7\mu\text{m}$.

- ☞ - temperature of Earth surface and stratosphere (top of atmosphere) for each site?
- is water vapor more important in Sahara or south of Irak?
- the thunderstorm cloud spectra has no atmosphere absorption bands. Why?

Simulating satellite signals: physical modeling of landscapes and radiative transfer

Vegetation/urban element

Tree, house, etc.

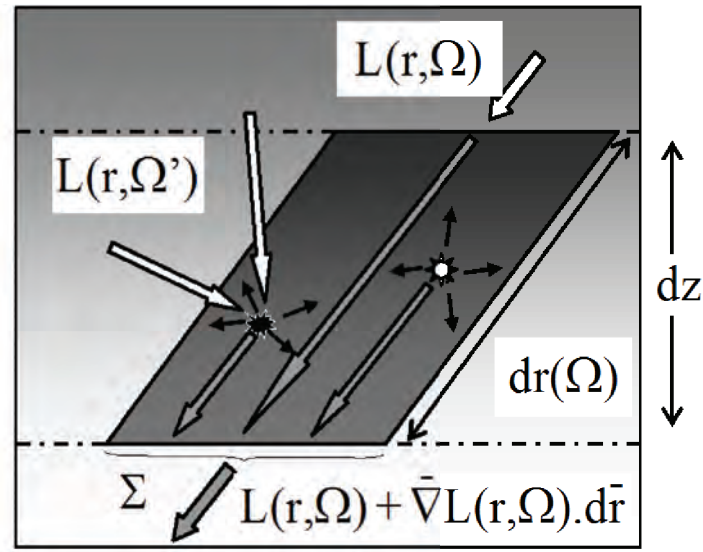
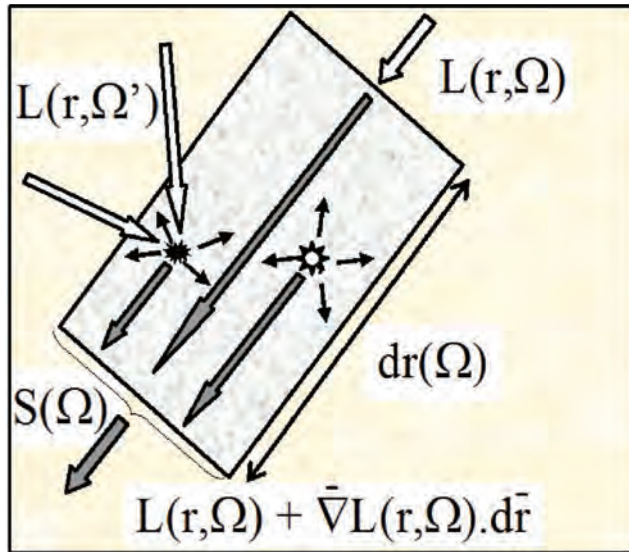
Vegetation/urban landscape

Leaf level: simple and complex models

Landscape level: simple/complex models

From Moreno (2014)


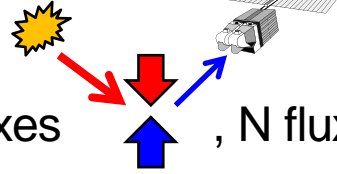
Simulating satellite signals: physical modeling of landscapes and radiative transfer



Radiative Transfer Equation (RTE):

$$\bar{\Omega} \cdot \bar{\nabla} L(r, \Omega) = -\alpha(r, \Omega) \cdot L(r, \Omega) + \int_{4\pi} L(r, \Omega') \cdot \alpha_d(r, \Omega' \rightarrow \Omega) \cdot d\Omega' + \mathcal{S}_{\text{emis}}(r, \Omega)$$

2 combined approaches to solve the RTE:

- **Simplified description of radiation:** 2 fluxes , 4 fluxes , N fluxes, ...

- **Simplified landscape description:** horizontal turbid layer



DART: 3D radiative transfer model

Principles:

- Landscape: - Turbid medium (fluid, veg., atm.) + Facets
 - Repetitive or isolated
 - Imported: BD_{atm} , L.C., 3D objects,...
- Discrete ordinates (space, directions)
- Earth / Atmosphere radiative coupling
- Iterative XS flux tracking (radiometer) or photon (Lidar)
- Parallel / projective projection \Rightarrow camera, pushbroom,...

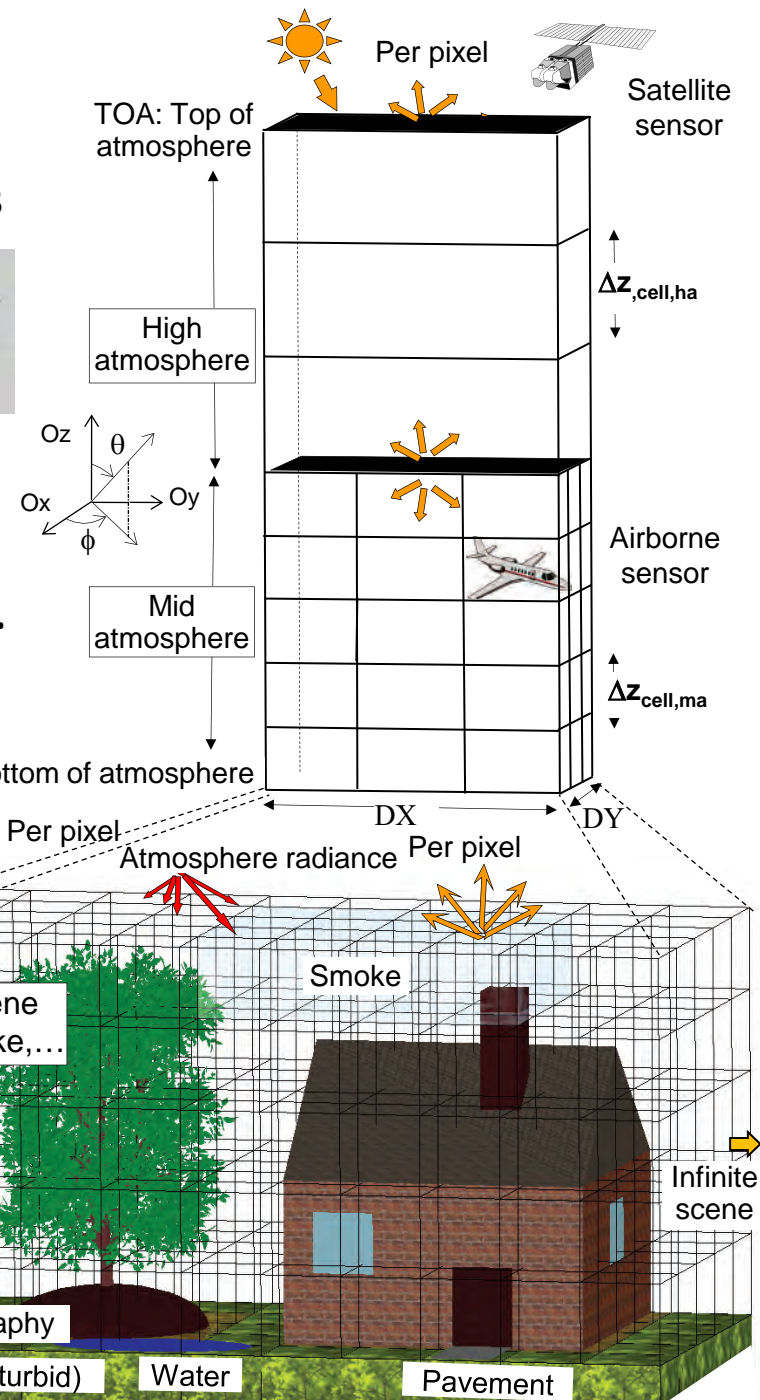


Operating modes

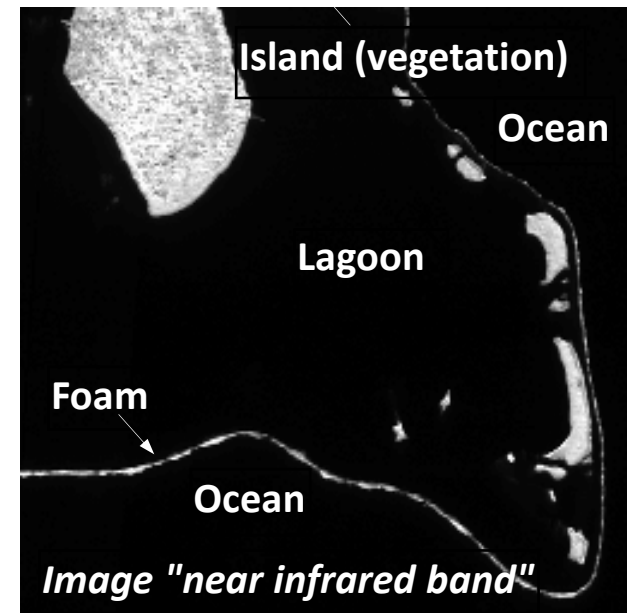
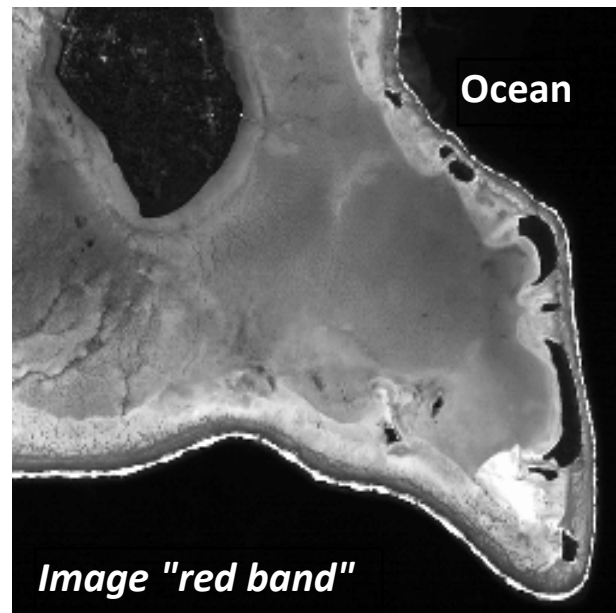
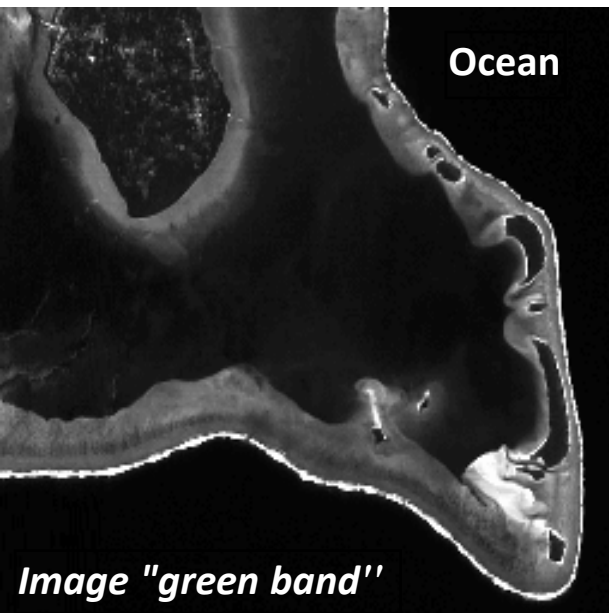
- Reflectance (R), Thermal (T) and (R+T)
- Lidar (RayCarlo: flux tracking + M. C.)
- Sequence of simulations \forall parameter (LAI, Ω_s, \dots)

Products

- Images $\rho_\lambda(\Omega_s, \Omega_v)$, $T_B(\Omega_s, \Omega_v)$, $L_\lambda(\Omega_s, \Omega_v) \forall \Omega_s, \Omega_v$
- Lidar waveform and photon counting
- 3D Radiative budget of Earth landscapes
- Atmosphere terms $\rho_{atm, \lambda}$, $T_{B, atm, \lambda}$, $L_{atm, \lambda}$



Spectral analysis: Aitutaki (Cook island) BOA radiance images (grey tone proportional to radiance)

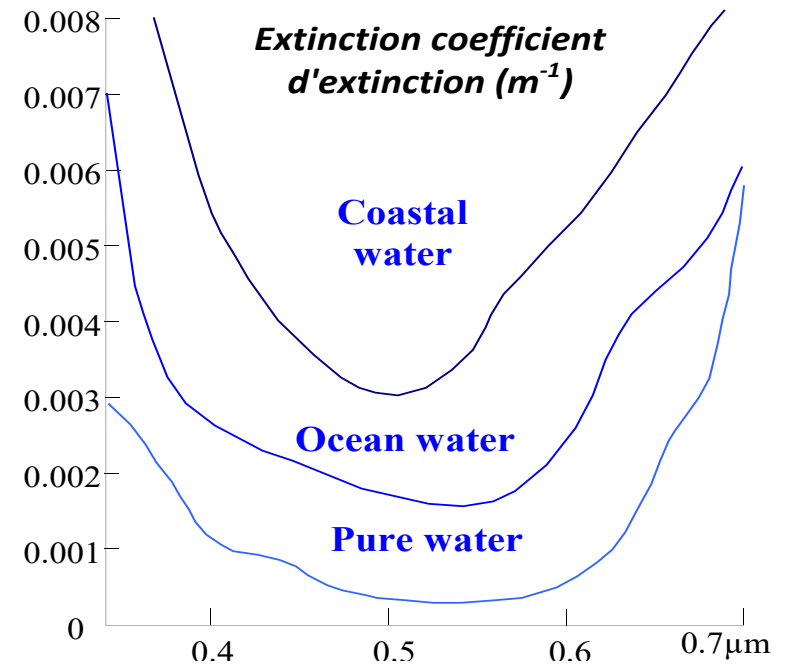
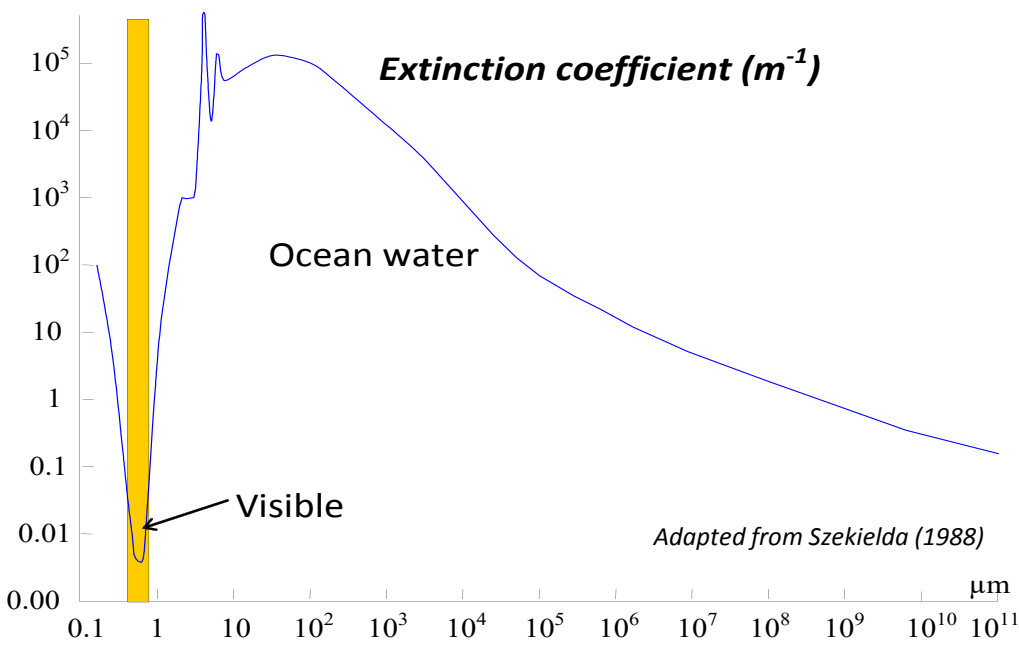
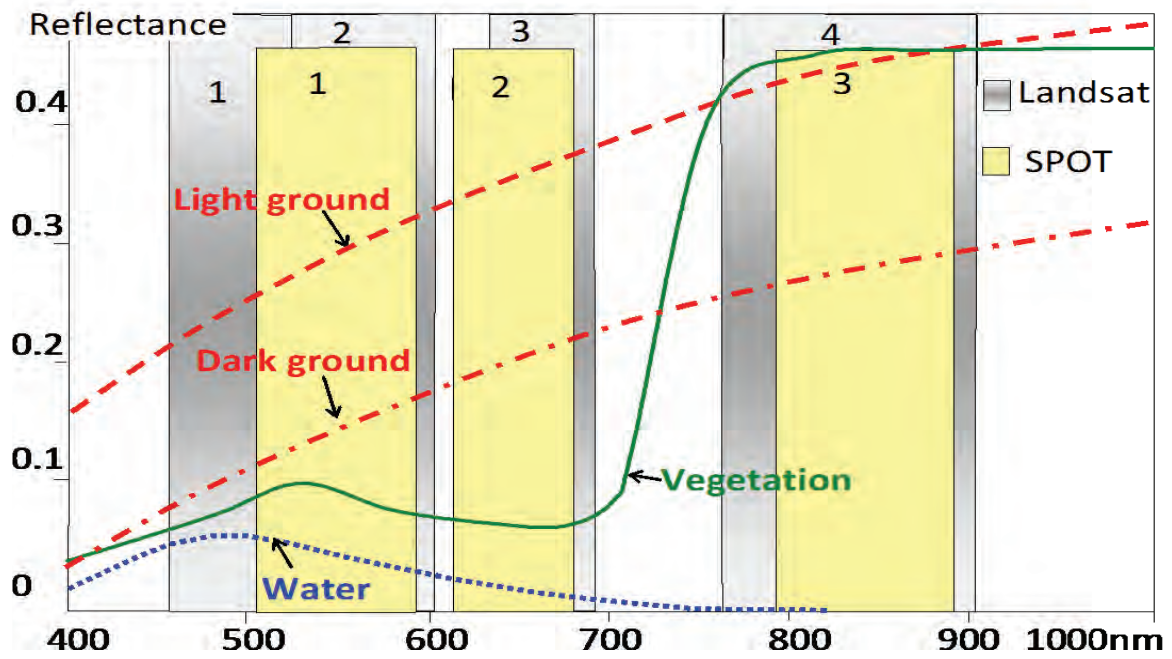


Hypotheses: same water in ocean & lagoon, vegetated islands.

Why :

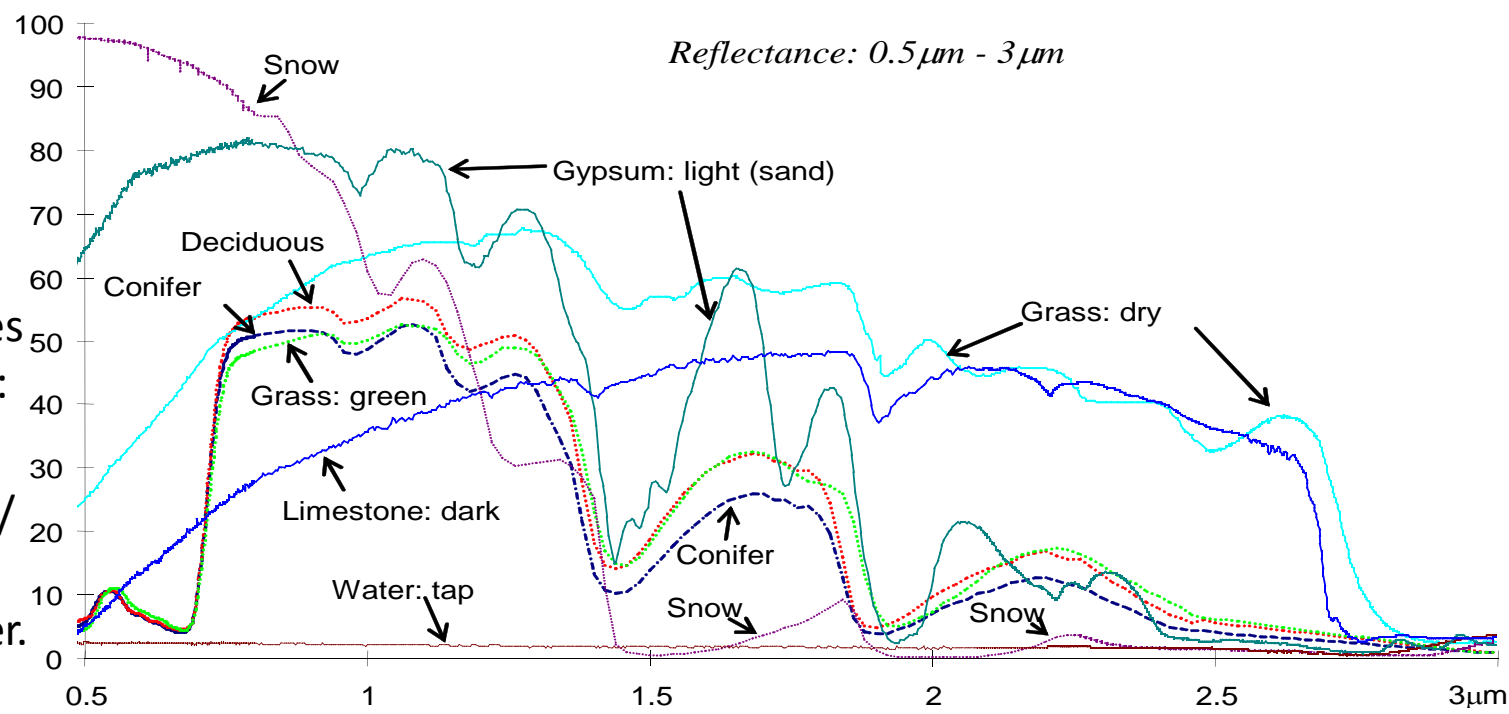
- Ocean: black tone in 3 images (blacker in NIR image)?
- Island: dark tone in "green" & "red", and light tone in "NIR"?
- Foam: light tone in 3 images, conversely to water surfaces?
- Lagoon: light tone in the "red", conversely to the ocean?

Spectral analysis: reflectance (ground, water, vegetation) and extinction coefficient (water)

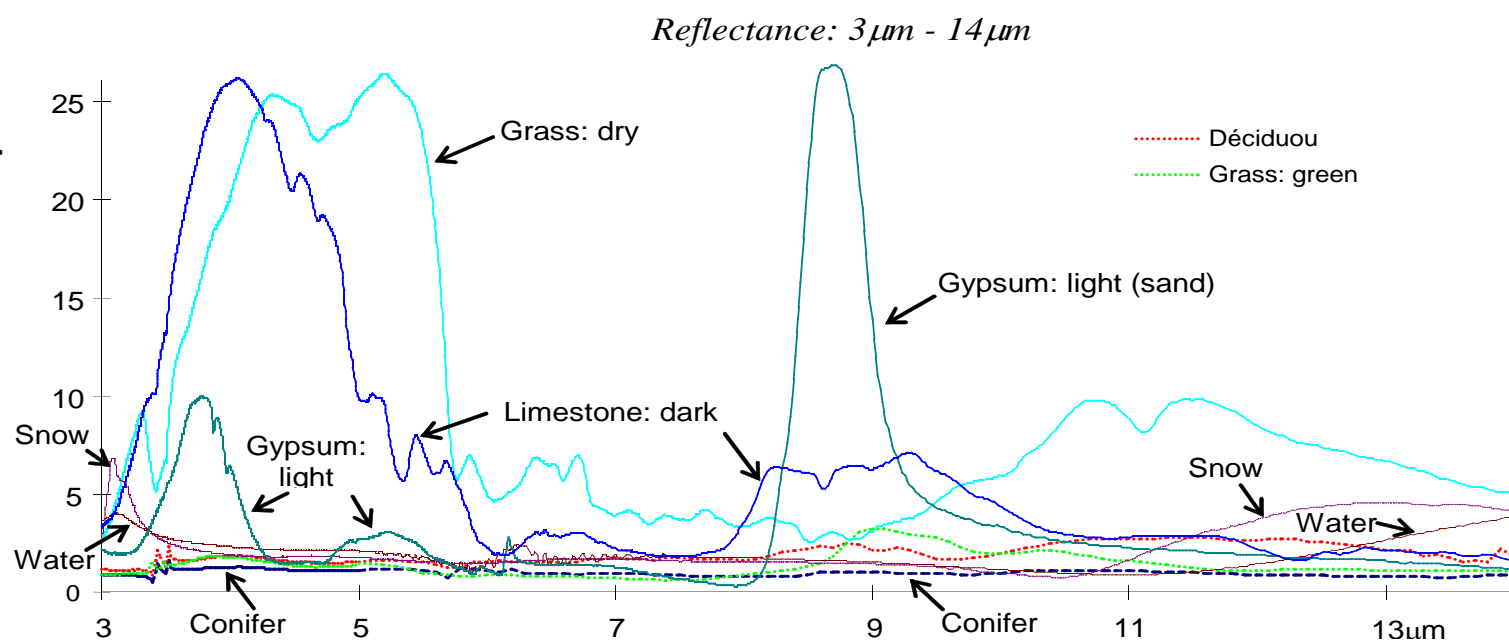


Spectral analysis: Optical properties of Earth surface elements

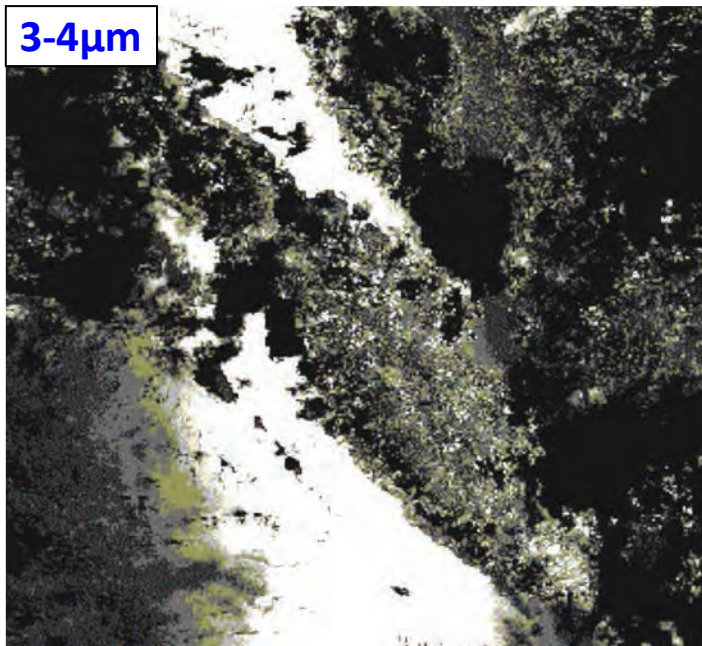
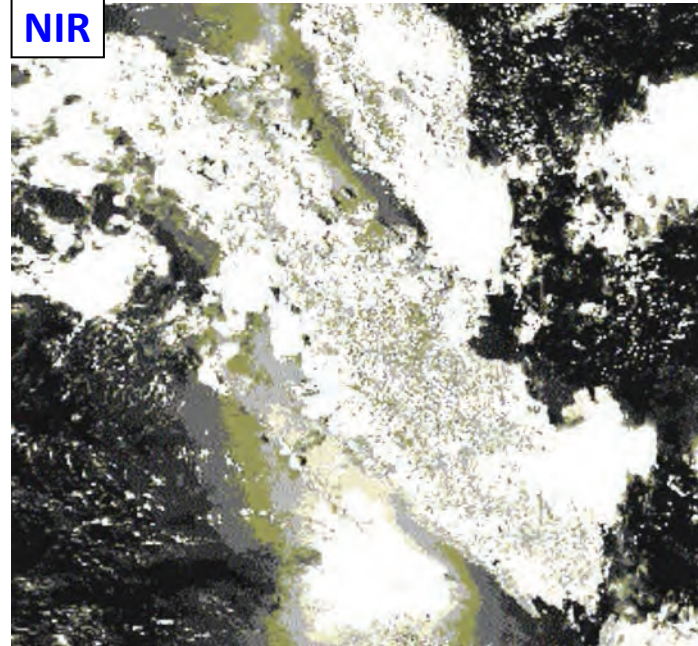
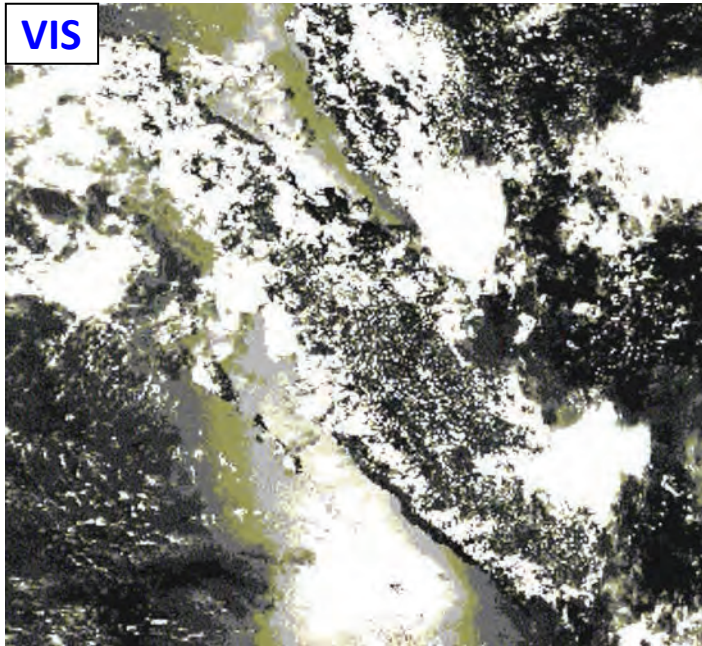
☠ Reflectance values are not equivalent: $\rho_{dd}(\lambda), \rho_{hd}(\lambda), \dots$
 Indeed, their view/illumination configurations differ.



☠ Condition of media: grinded/dried ground, etc.



Spectral analysis: NOAA images (grey tone proportional to radiance) – Sumatra island, 1993



Why:

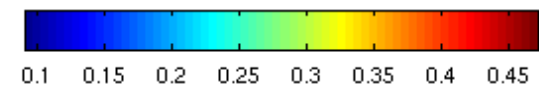
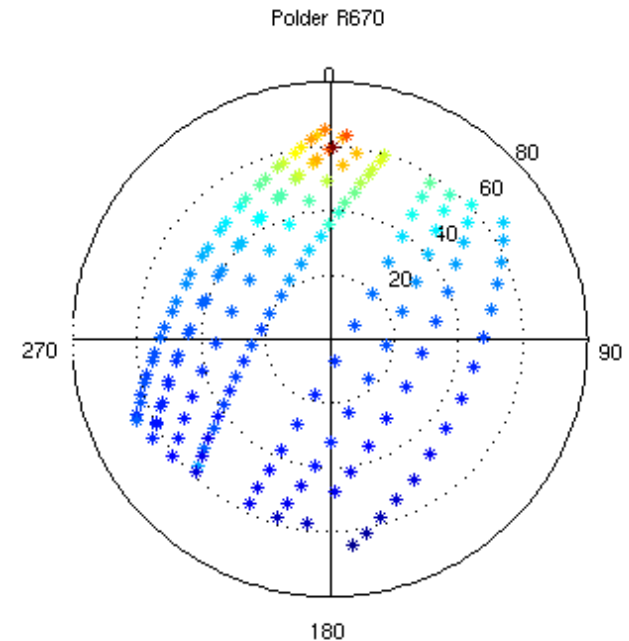
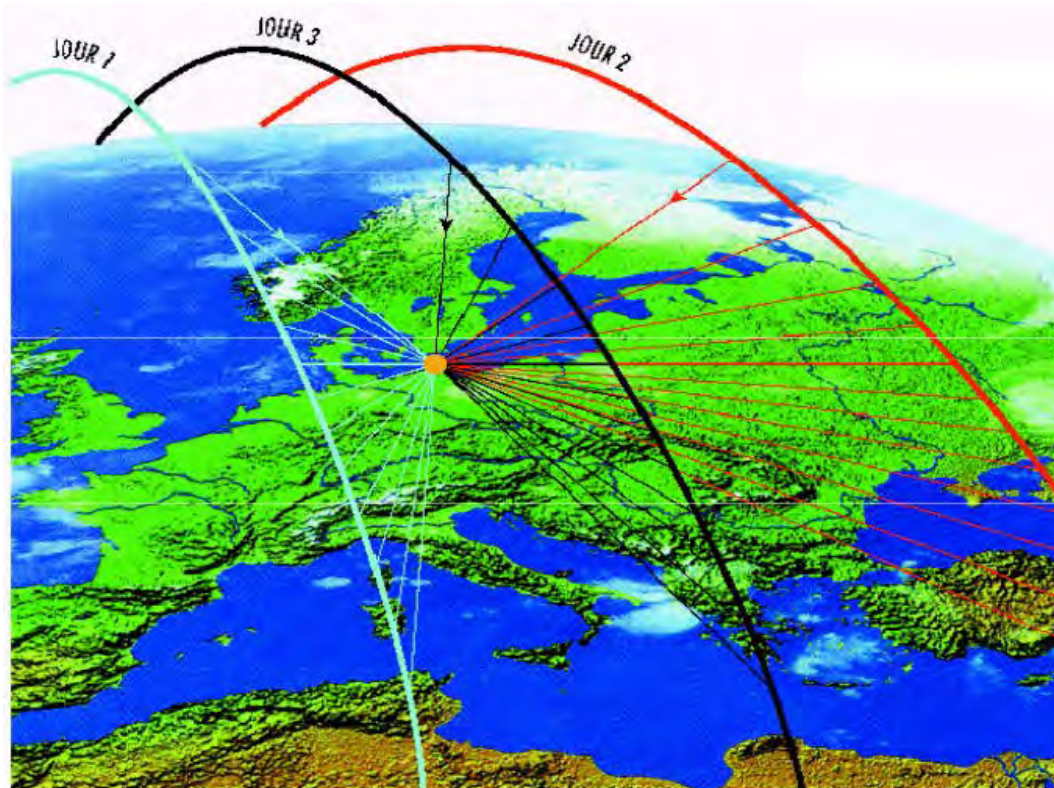
- Sumatra has dark tones in the VIS image and light tones in the NIR image?
- Clouds have light tones in the VIS image and dark tones in the "3-4 μ m" image
- In the VIS image, the bright spot below South Sumatra is not a cloud. What is it?

View direction: POLDER (Polarization and Directionality of Earth Reflectances) - 114° FOV, 6km

The anisotropy of the Earth surfaces reflectance ρ strongly affects TOA radiance.

ρ : described by BRDF or Bidirectional Reflectance Distribution Function (BRDF)

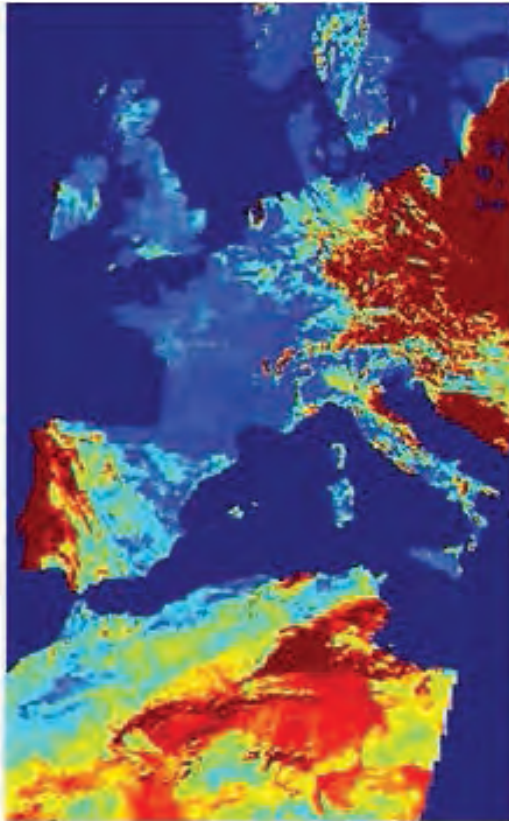
BRDF = function of sun direction (θ_s, ϕ_s) & view direction (θ_v, ϕ_v) . In practice: $\rho(\theta_s, \theta_v, \phi_s - \phi_v)$



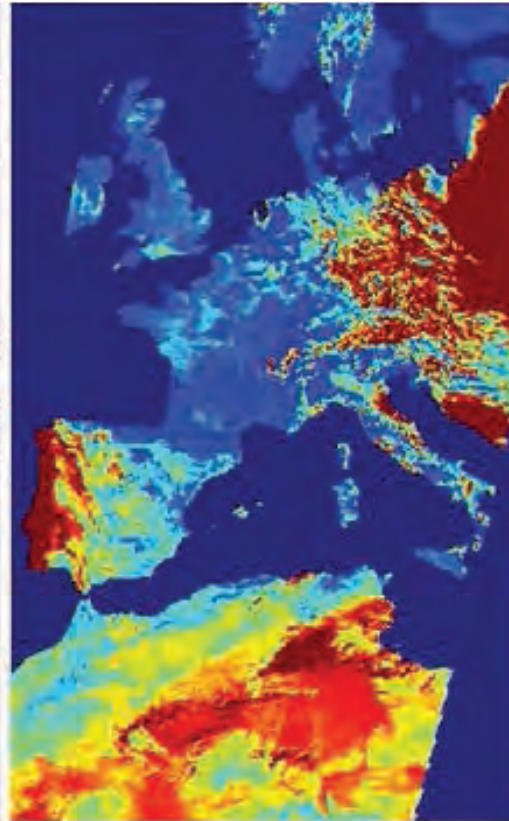
(E. Vermote, C. Justice and Breon, NASA supported Land LTDR Project)

View direction: POLDER (16/09/96) - 670nm - 114° FOV

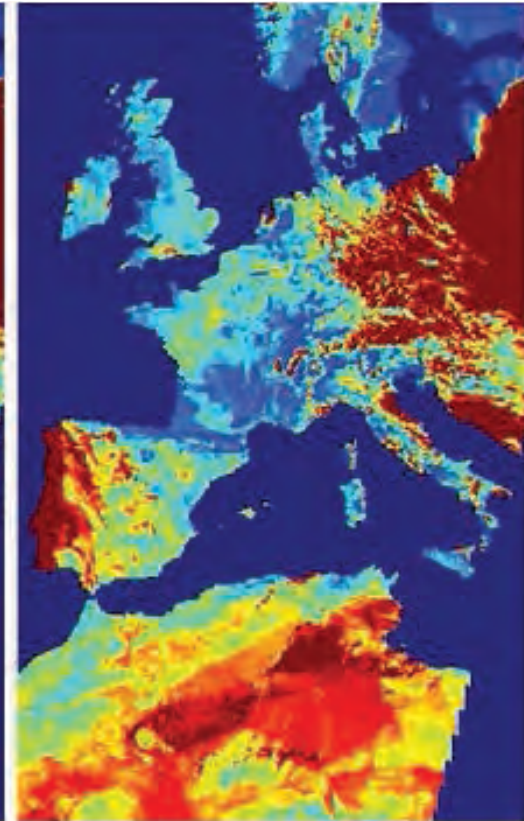
Back



Nadir



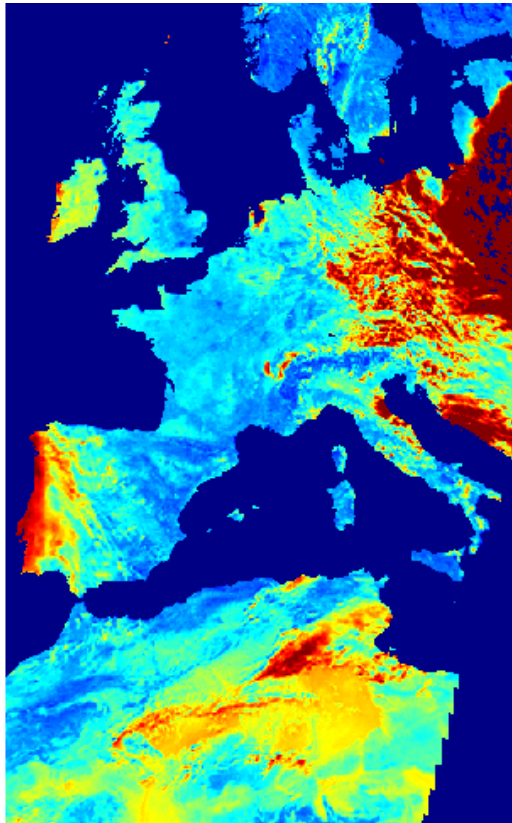
Forward



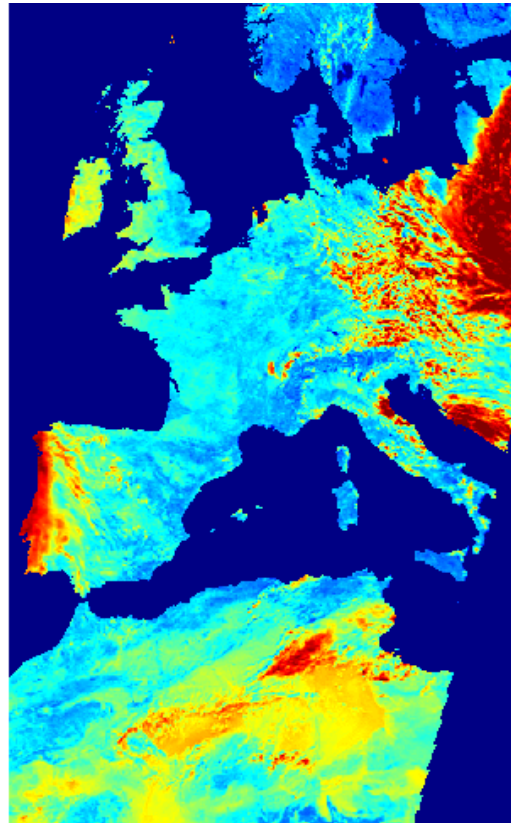
- ☞ Which elements do have the larger reflectance value (reddish tones)?
- ☞ Why does reflectance change with view direction with a maximum in the forward direction?

View direction: POLDER (16/09/96) - 865nm - 114° FOV

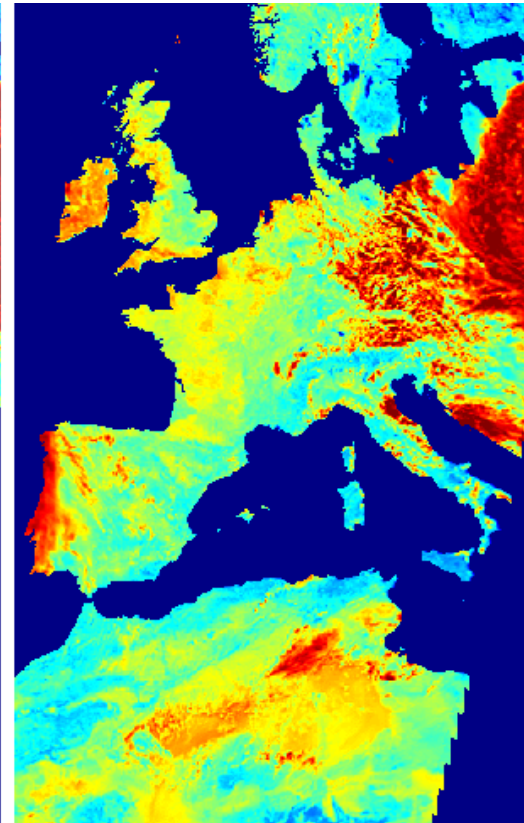
Back



Nadir



Forward

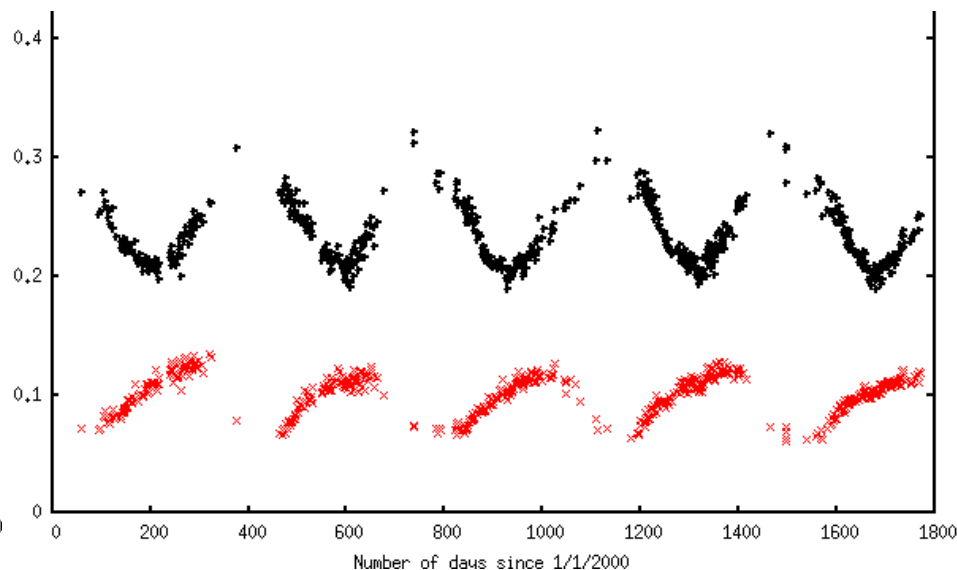
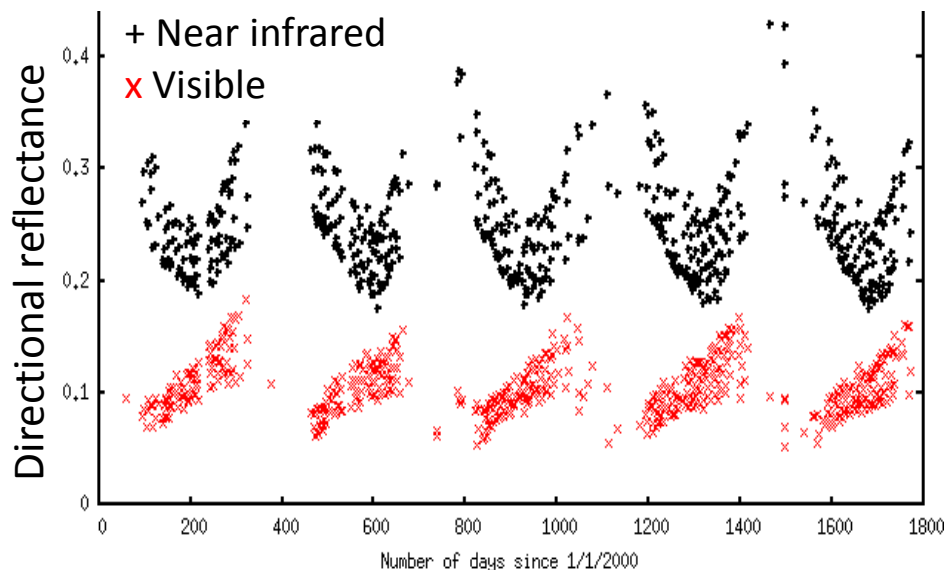


☞ For which configuration, a schematic landscape {bare ground + trees} has a strongly anisotropic reflectance with a maximum at nadir. Same, with minimum at nadir.

MODIS daily VIS / NIR surface reflectance: south Africa tropical savanna, 2000-2004

Not normalized reflectance

Normalized reflectance: BRDF model calibrated with POLDER data



(E. Vermote, C. Justice and Breon,
NASA supported Land LTDR Project)

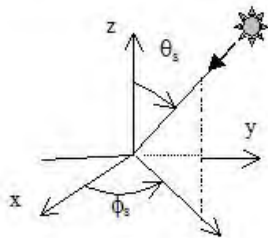
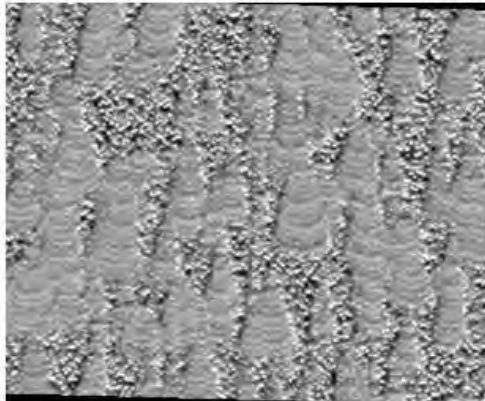
☞ Does the variability of Earth surface reflectance increase or decrease if satellite spatial resolution coarsens?

Reflectance anisotropy with view direction: verification with RS model

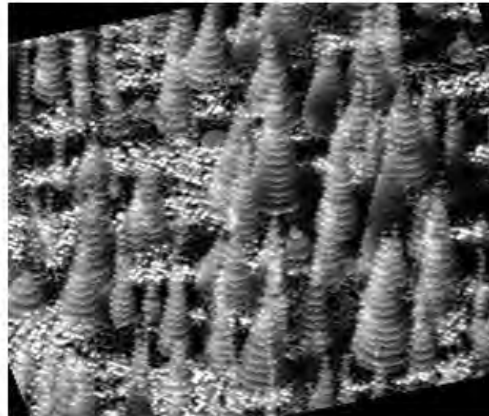
OLD BLACK SPRUCE

- DART SIMULATIONS: NIR -

Hot spot ($\rho_{\text{PIR}} \approx 0.287, \theta_v = 35^\circ, \phi_v = 0^\circ$)

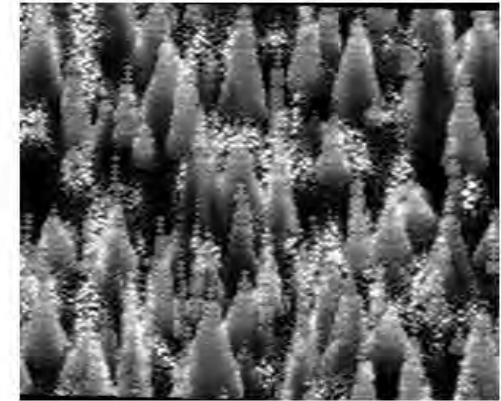
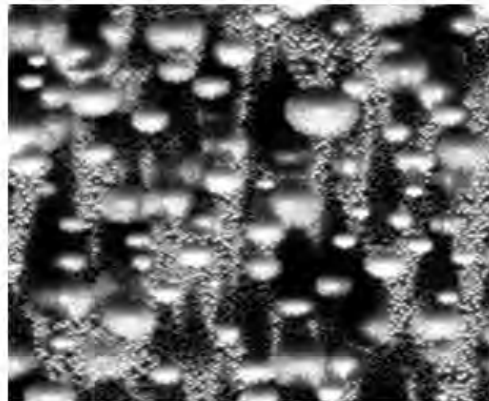


Sun direction: $\theta_s = 35^\circ, \phi_s = 0^\circ$



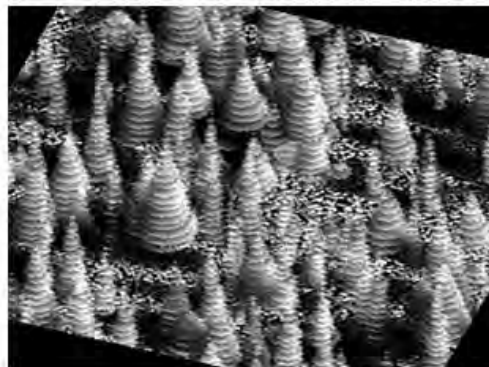
($\rho_{\text{PIR}} \approx 0.168, \theta_v = 35^\circ, \phi_v = 72^\circ$)

($\rho_{\text{PIR}} \approx 0.156, \theta_v = 35^\circ, \phi_v = 180^\circ$)



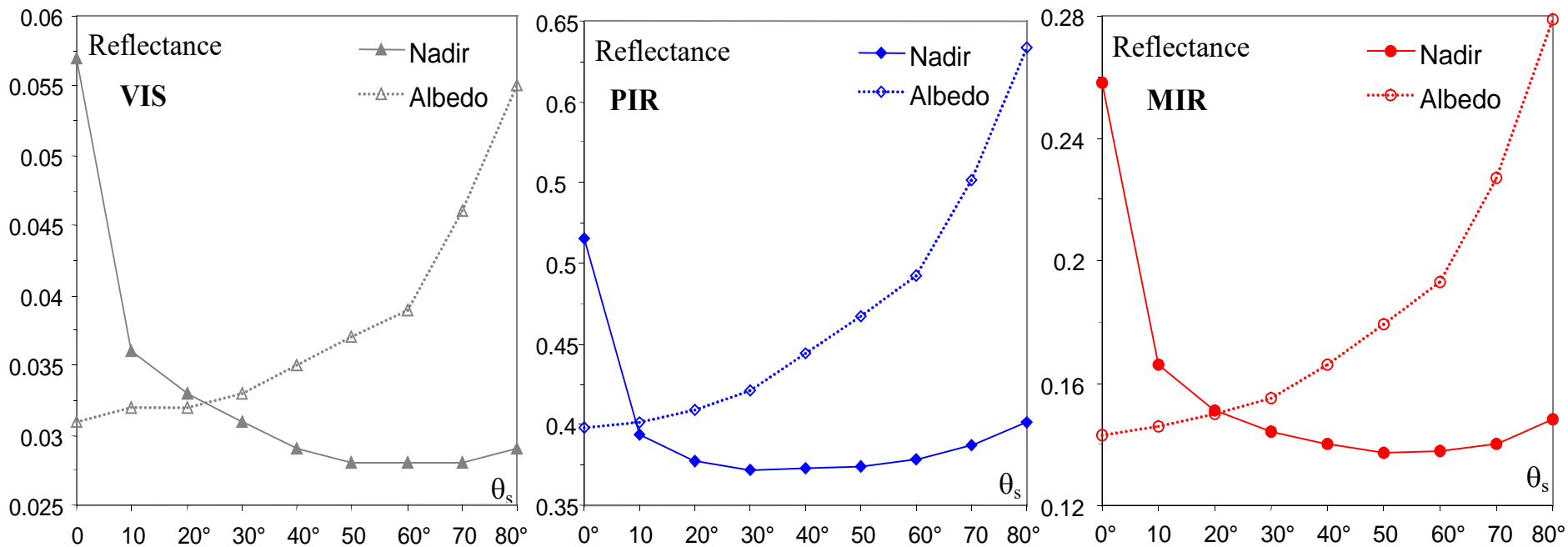
Nadir ($\rho_{\text{PIR}} \approx 0.147, \theta_v = 0^\circ$)

($\rho_{\text{PIR}} \approx 0.173, \theta_v = 35^\circ, \phi_v = 288^\circ$)



Reflectance varies from
0.147 to 0.287!!!

Reflectance and albedo anisotropy with sun direction: verification with RS model

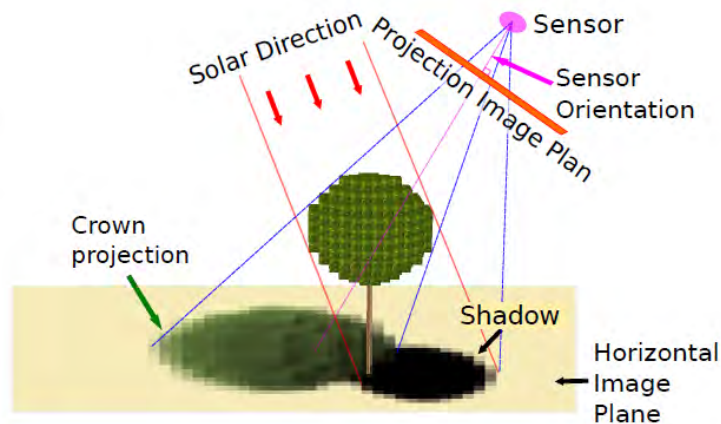
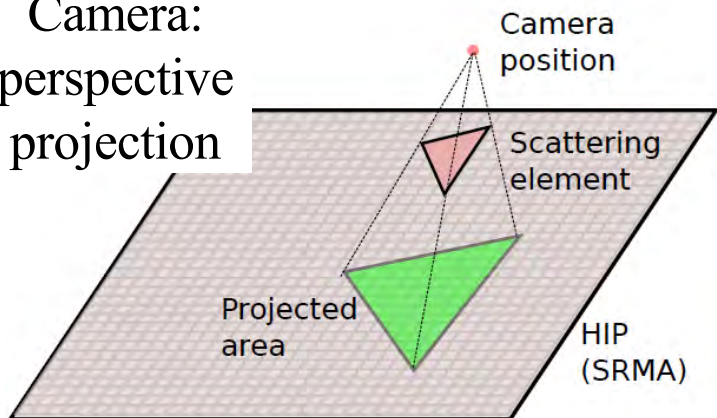


DART simulations

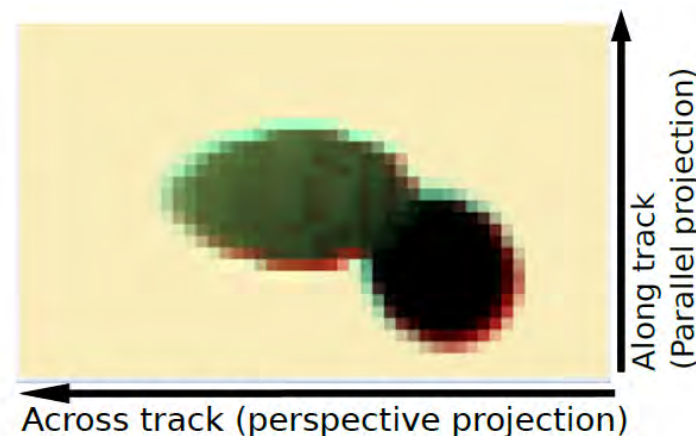
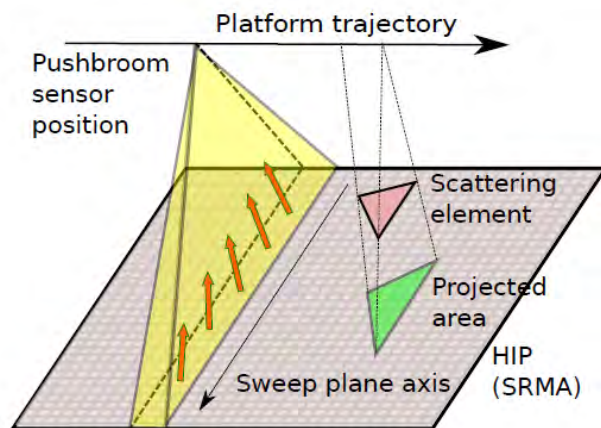
☞ Nadir reflectance and albedo values can differ a lot. Hence, to approximate the Earth surface albedo as a directional reflectance value can be a large source of error.

Satellite and airborne sensors with finite FOV (perspective and parallel-perspective projections)

Camera:
perspective
projection



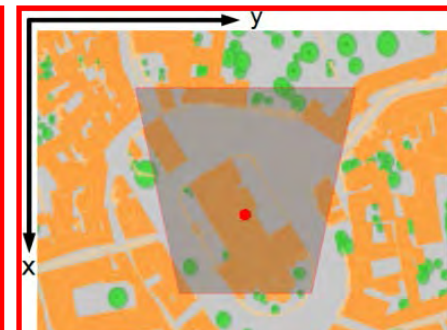
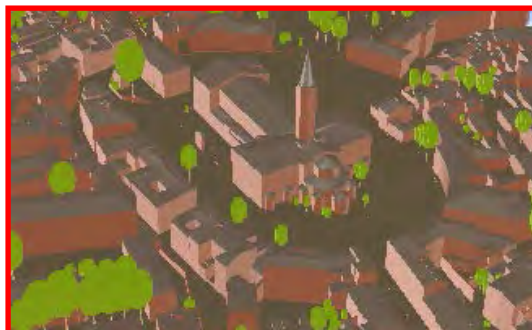
Pushbroom: parallel-
perspective projection



Non-zero FOV impacts RS data: **geometric distortion** + **view direction difference**

Example of geometric distortion: Basilica St-Sernin (Toulouse, France)

Identical objects in a simulated landscape appear differently, depending on view configuration (distance, view angle)



Toulouse urban data base - DART scene



DART simulated images

Parallel projection (satellite, $\theta_v=50^\circ$, $\phi_v=0^\circ$)

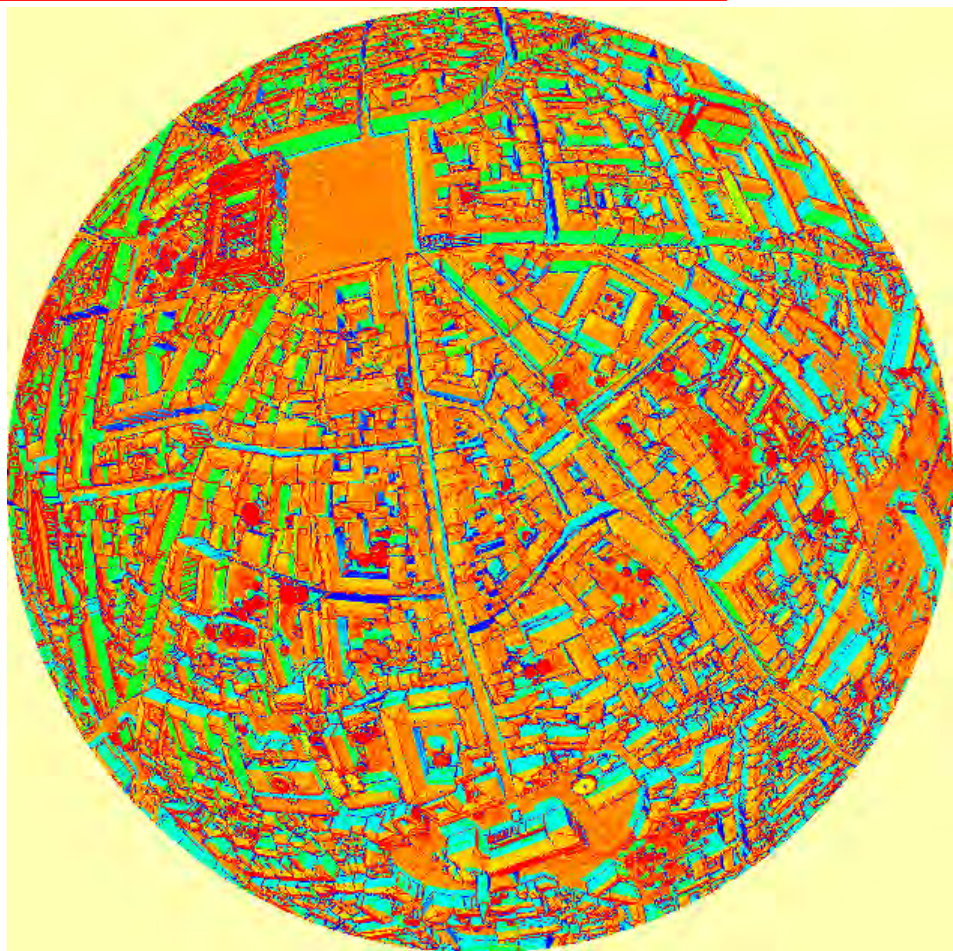
Perspective projection (UAV camera, $z_s=140\text{m}$)

Radiance variability due to geometry: fish eye camera VIS/TIR images (Toulouse)

Why does radiance change with view direction in the VIS/NIR? In the TIR?



RGB color composite

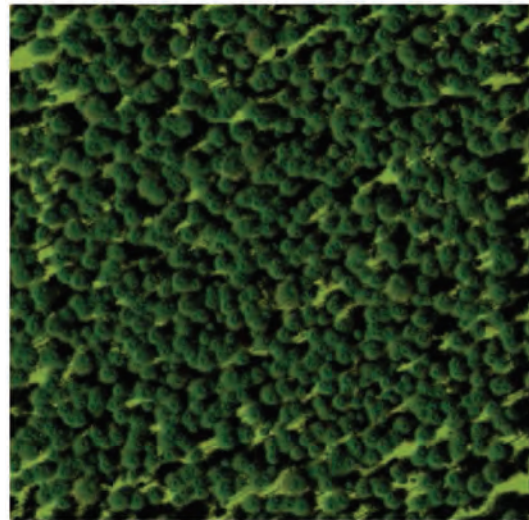


- Thermal infrared camera image
(DART simulated images)

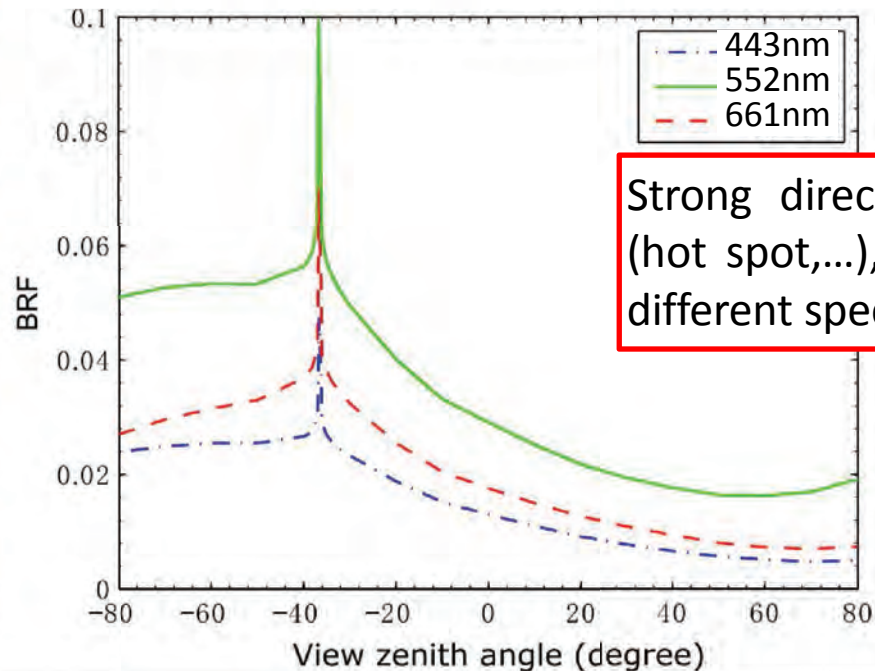
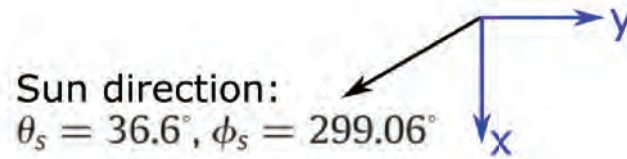
Satellite sensor with FOV=0 (parallel projection) - Järvselja pine stand, Estonia (RAMI4)



simulated scene



nadir-view image

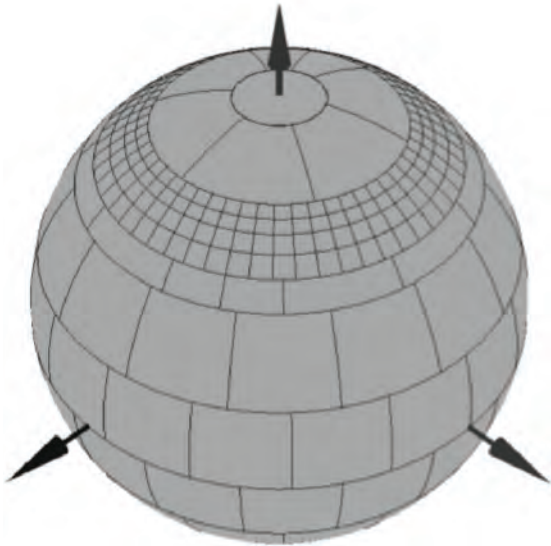


Strong directional effects (hot spot,...), different for different spectral bands.

Satellite / airborne sensor with finite FOV (perspective projection) - Järvselja pine stand, Estonia

Direction oversampling within camera FOV

UAV camera ($\theta_v = 50^\circ$, $z_s = 140m$)



Identical objects (trees,...) appear with different radiance values due to sensor FOV (angular effects)

Hot spot effect in actual airborne and satellite images



Camera ¹



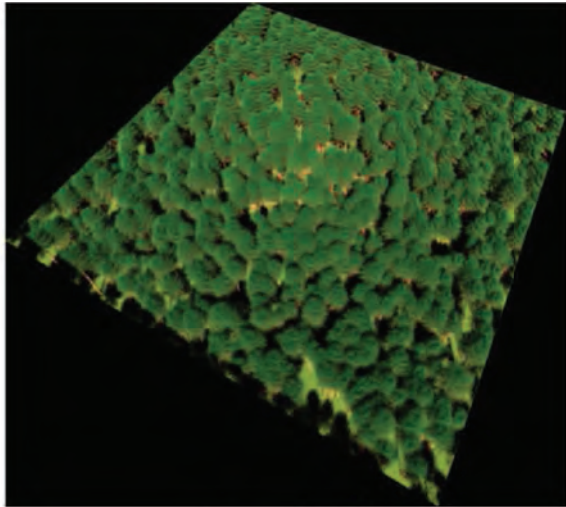
MODIS image (October 27, 2002 ²)

- Usually, sun-sensor geometry impacts strongly vegetation reflectance anisotropy.
- Important role of hot spot (perception of within vegetation shadows).

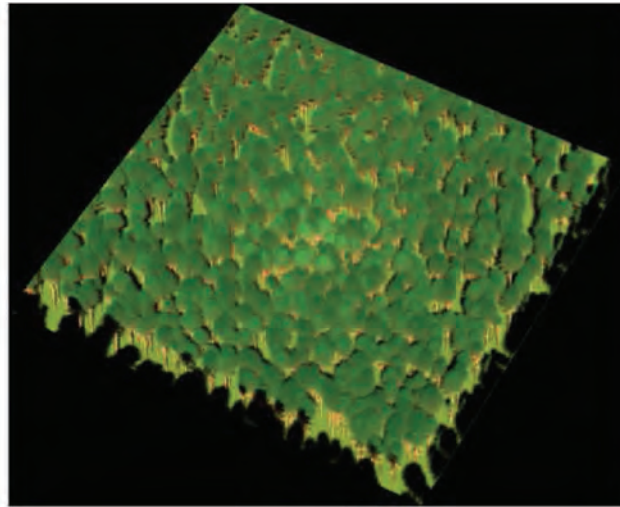
1. <http://academic.emporia.edu/aberjame/remote/lec10/hotspot.jpg>

2. <http://earthobservatory.nasa.gov/IOTD/view.php?id=83048>

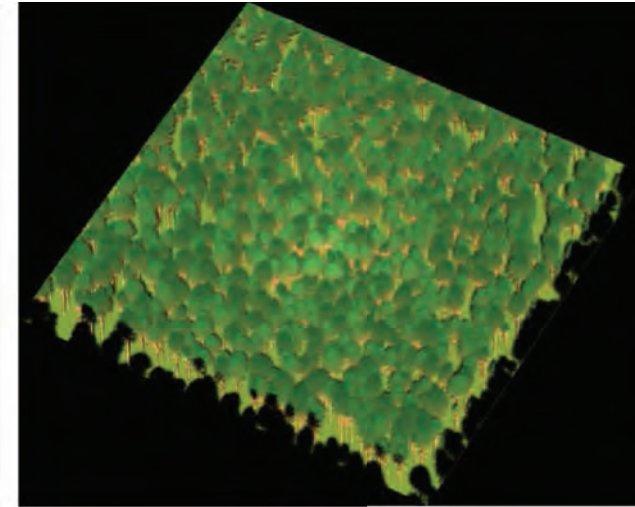
Camera hot spot effect at different altitudes



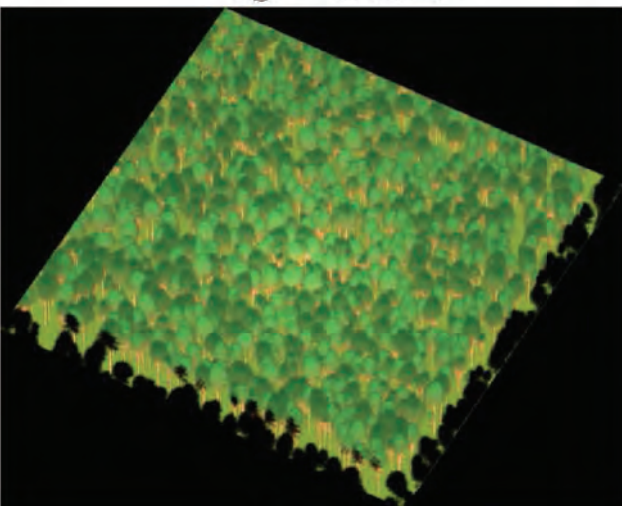
$z_S = 0.1km$



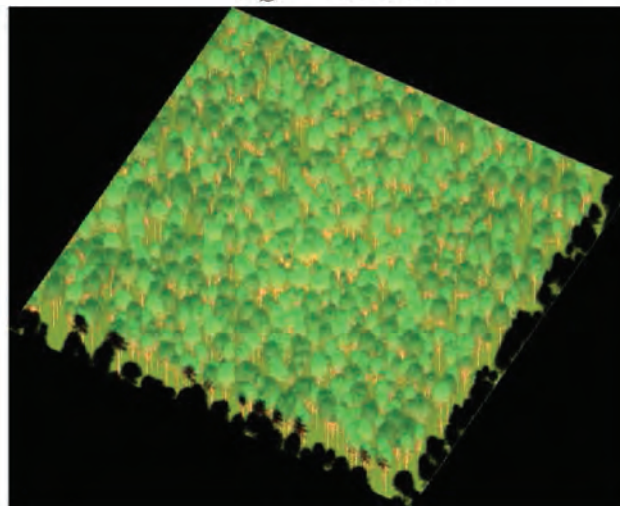
$z_S = 0.5km$



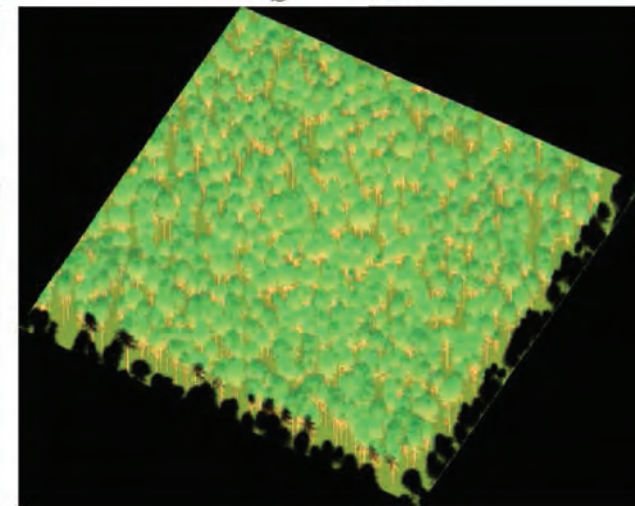
$z_S = 1km$



$z_S = 5km$



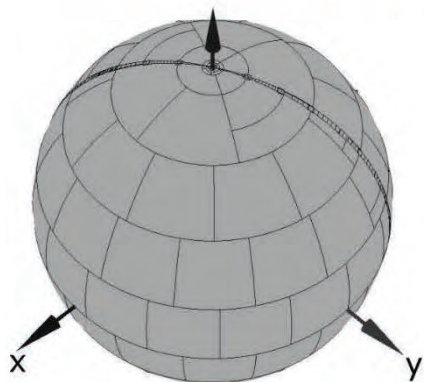
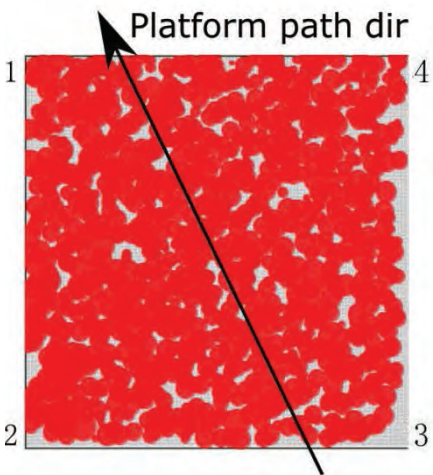
$z_S = 50km$



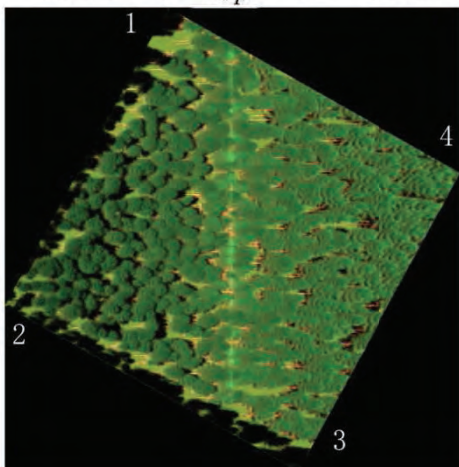
$z_S = 500km$

Pushbroom hot spot effect at different altitudes

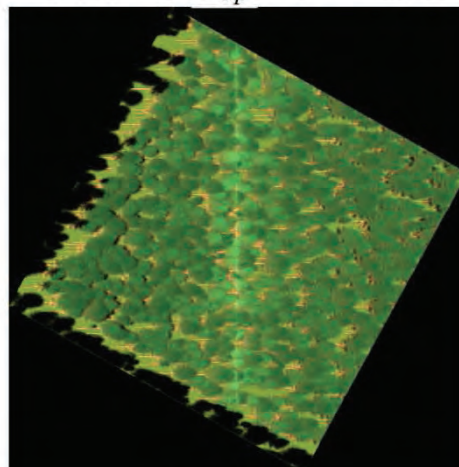
Sun direction:
 $\theta_s = 36.6^\circ$, $\phi_s = 299.06^\circ$



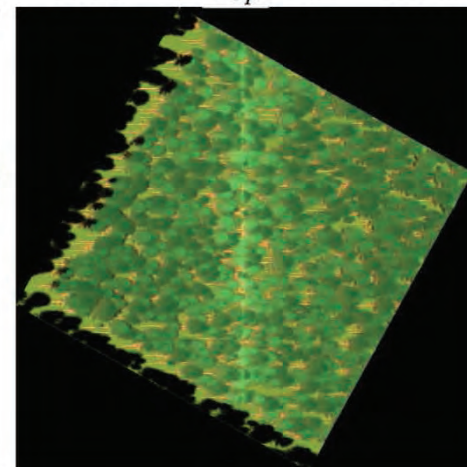
$-12.31^\circ \leftarrow \theta_{vp} \rightarrow -55.44^\circ$
 $-31.23^\circ \leftarrow \theta_{vp} \rightarrow -41.44^\circ$
 $-33.98^\circ \leftarrow \theta_{vp} \rightarrow -39.10^\circ$



$z_S = 0.1km$

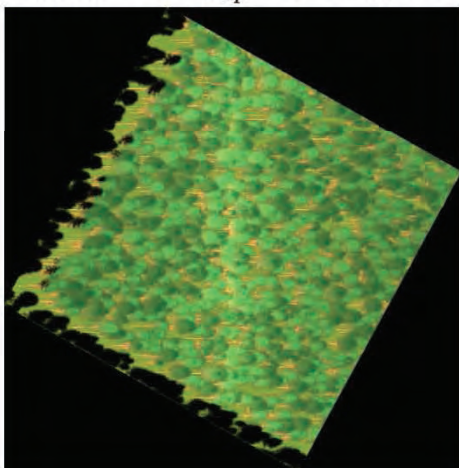


$z_S = 0.5km$



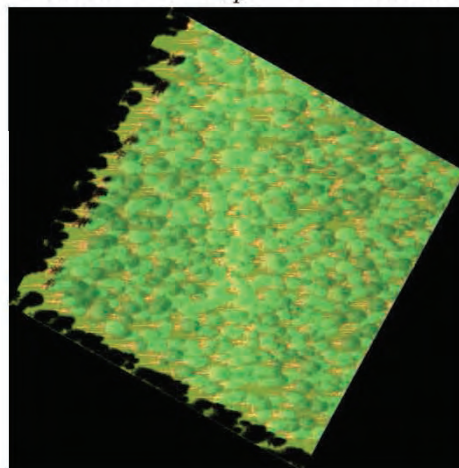
$z_S = 1km$

$-36.09^\circ \leftarrow \theta_{vp} \rightarrow -37.11^\circ$



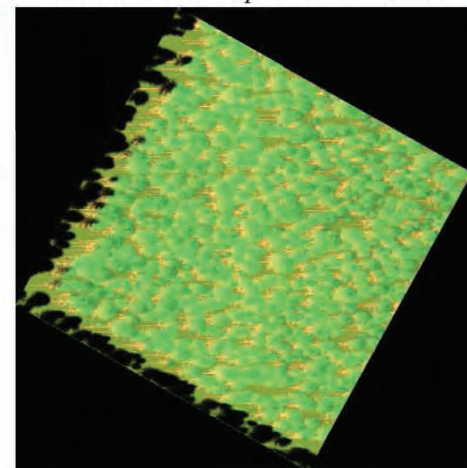
$z_S = 5km$

$-36.55^\circ \leftarrow \theta_{vp} \rightarrow -36.65^\circ$



$z_S = 50km$

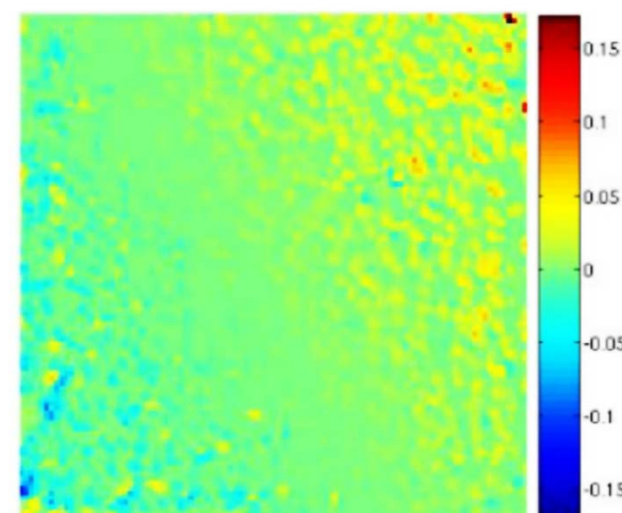
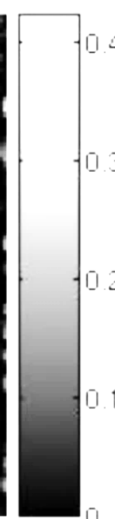
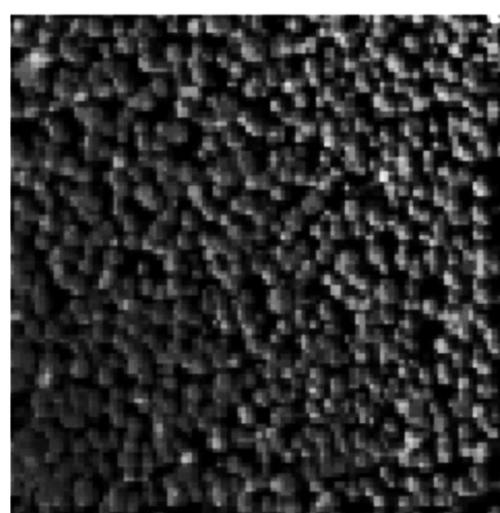
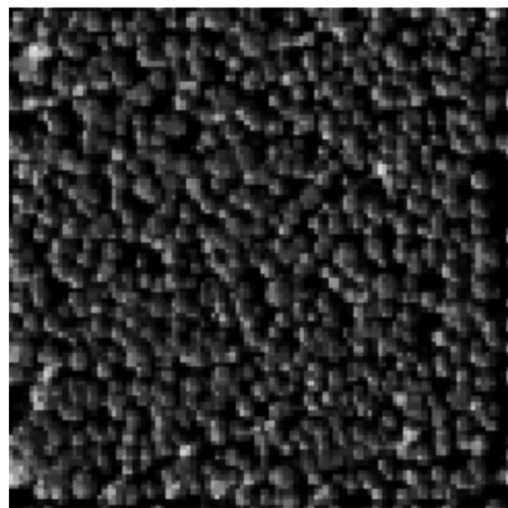
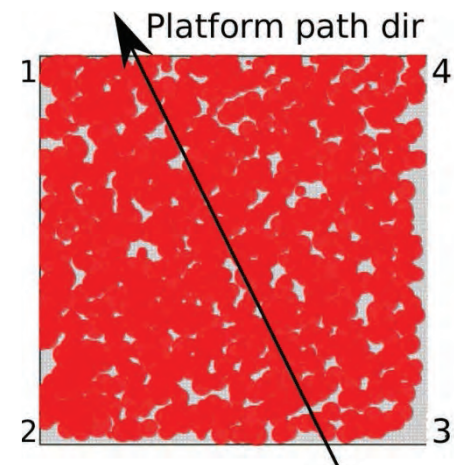
$-36.59^\circ \leftarrow \theta_{vp} \rightarrow -36.61^\circ$



$z_S = 500km$

Pixel-wise comparison: ortho-rectified images of satellite and airborne pushbroom imagers

- 552nm
- Altitude: 200m
- Central zenith angle: -20°



Parallel projection image

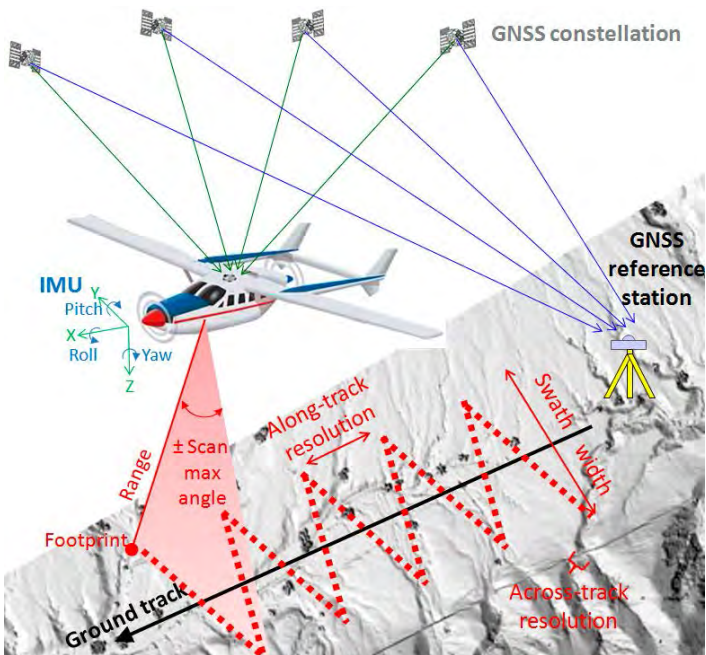
Pushbroom image

Difference image:
pushbroom - parallel projection

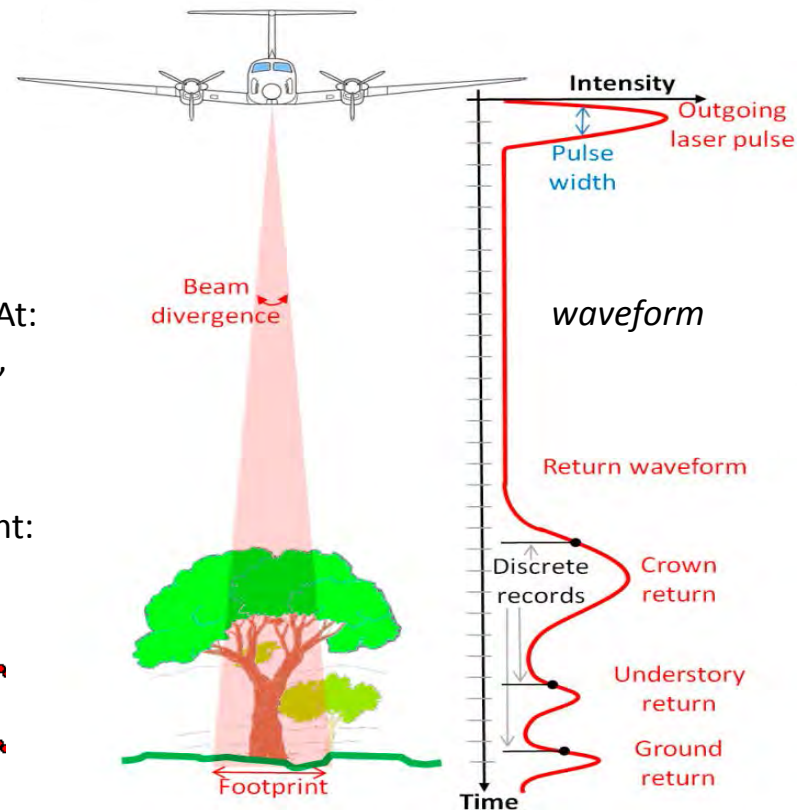
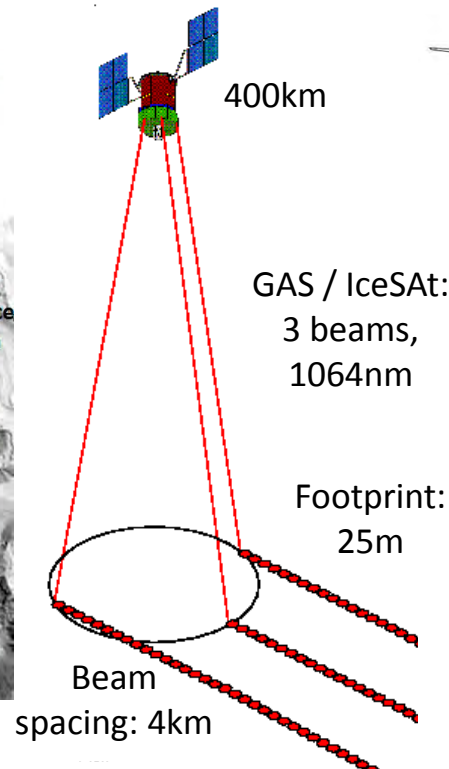
Light Detection And Ranging (LiDAR)

LiDAR emits laser pulse, and uses the time-of-flight technique for measuring distance and amplitude of return energy. Satellite, airborne and terrestrial systems

Various types: discrete-return, waveform and photon counting LiDARs.



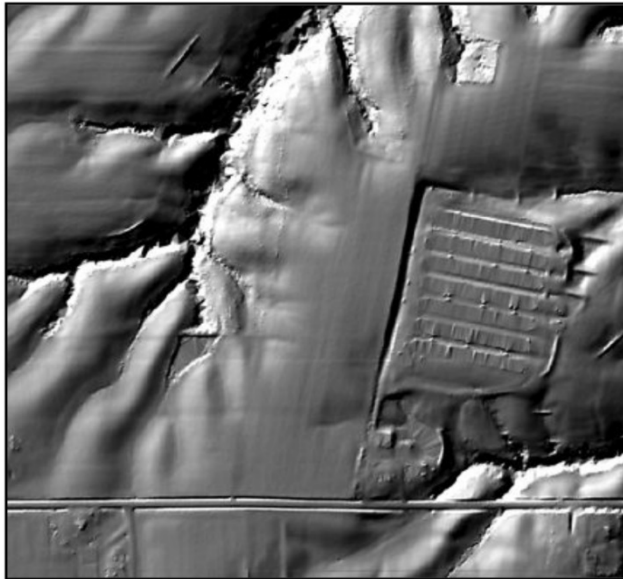
Fernandez-Diaz (Remote Sensing, 2014)



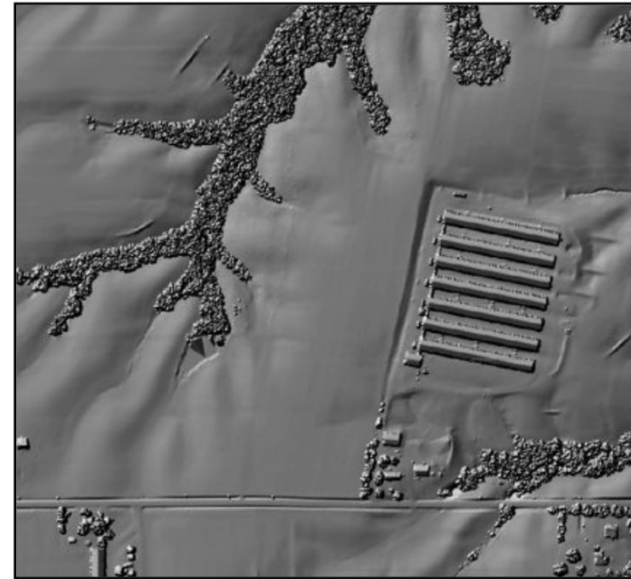
Light Detection And Ranging (LiDAR)

Application: DEM/DSM, vegetation / urban architecture & dimensions, atmosphere,...

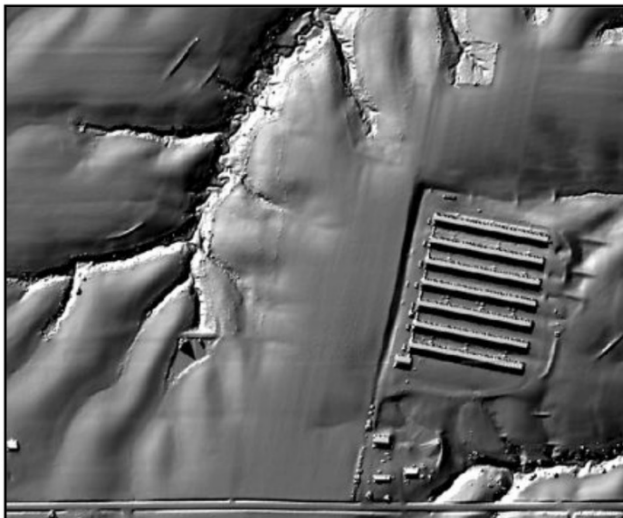
DEM



First return



Last return



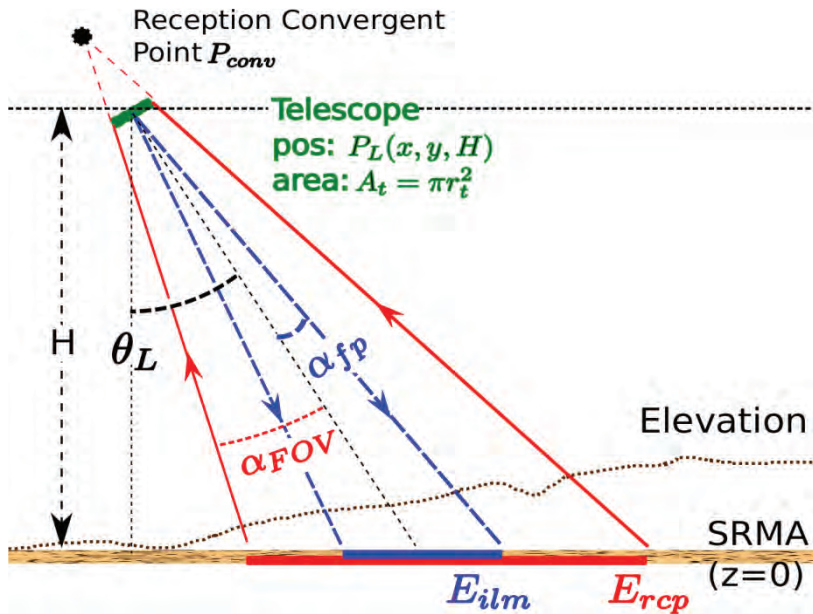
Intensity



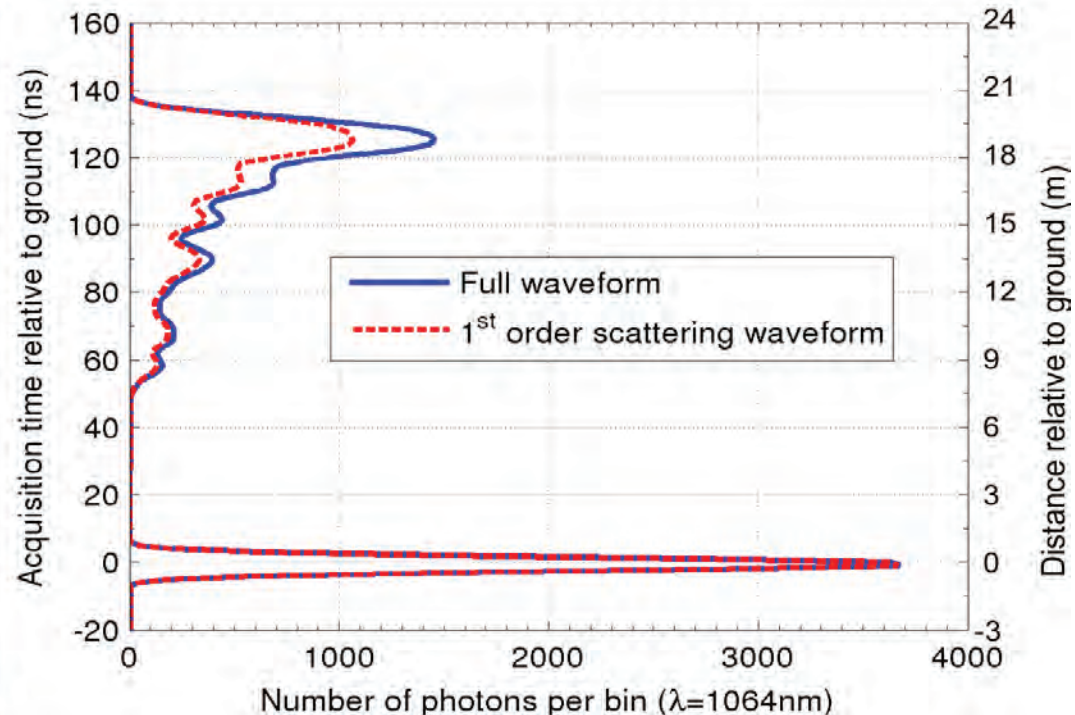
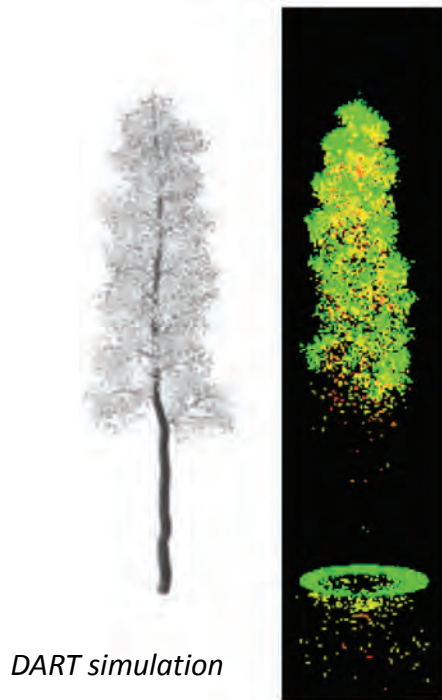
1st order LiDAR models: Geo-optical models with **hot spot** configuration.

Multiple order models: Monte-Carlo ray tracing (Flight, DELiS,...), DART (quasi-MC),...

Small footprint waveform simulation: Linden tree from RAMI-4 ($\lambda = 1064\text{nm}$, $H = 10\text{km}$)

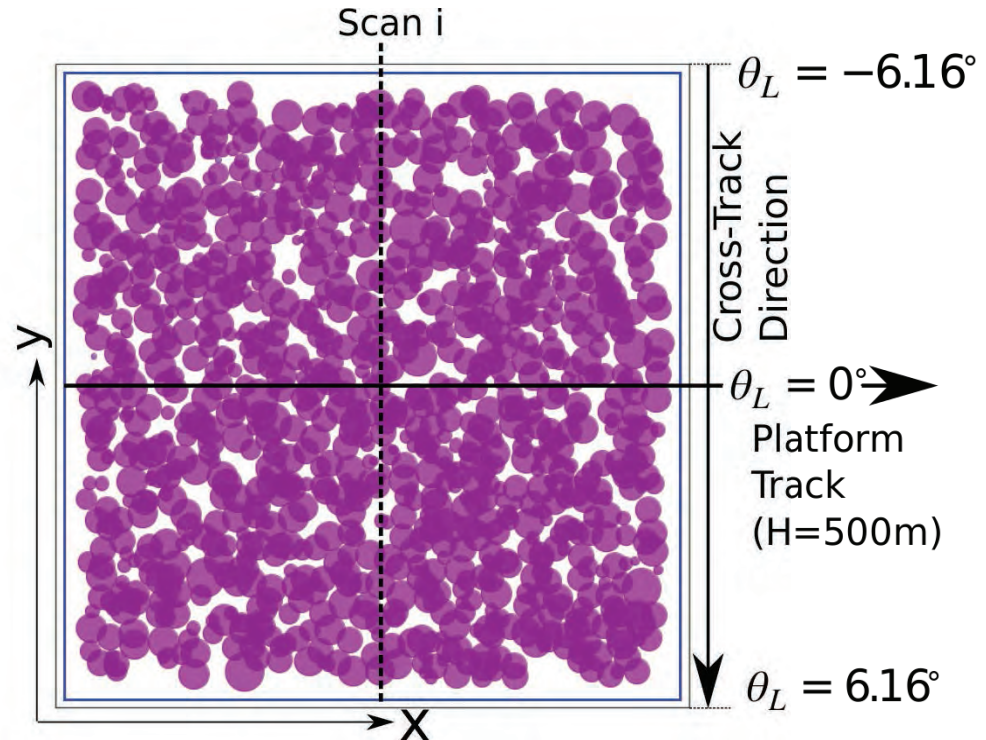


Parameters	Symbols	Values
Sensor area	A_t	0.1m^2
Time step per bin	δt_{bin}	1 ns
Footprint divergence half angle	β_{fpp}	0.25 mrad
FOV divergence half angle	β_{FOV}	0.4 mrad



ALS simulation: LiDAR of CAO AtoMS system over Järvselja pine stand (RAMI-4)

Parameters	Values
Sensor area	0.1m ²
Wavelength	1064 nm
Pulse energy	1 mJ
Time step per bin	1 ns
Distance step per bin	30 cm
Footprint divergence half angle	0.25 mrad
FOV divergence half angle	0.4 mrad
Pulse Repetition Frequency	400 kHz
Scan frequency	140 Hz
Maximum look angle	32.5 °
Platform speed	49 m/s (95.24 knots)
Along-track distance step per scan	0.35 m
Look angle step per pulse	0.02275 °

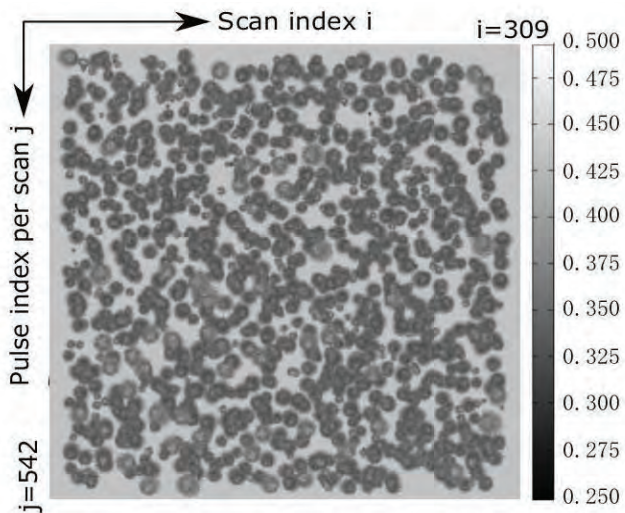


Number of pulses: 167478 (309 scans \times 542 pulses per scan)

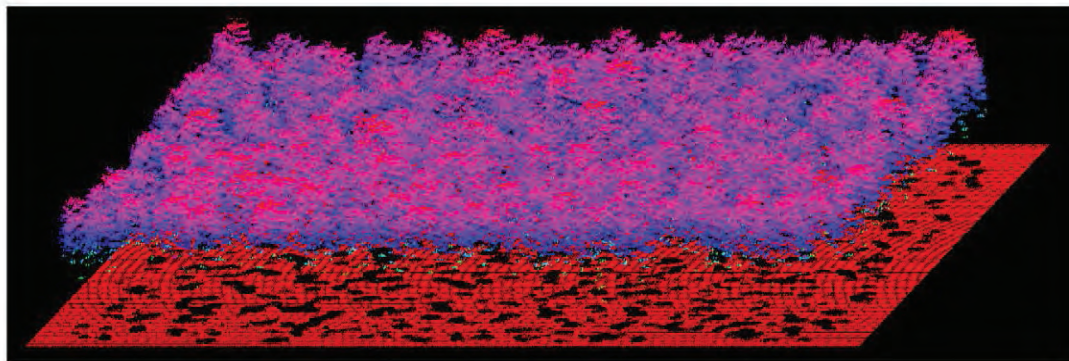
Pulse density: 14.35 /m²

5000 SPs per pulse \rightarrow 0.78 seconds / pulse / thread \Rightarrow 110 minutes with 20 threads

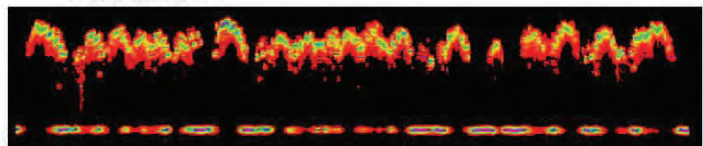
ALS simulation: LiDAR of CAO AtoMS system over Järvselja pine stand (RAMI-4)



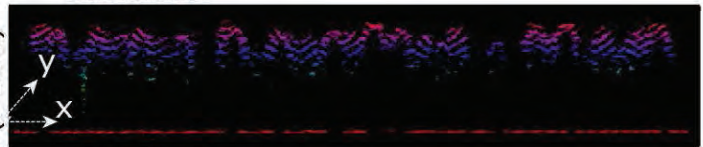
Display of DART simulations with SpDLib code



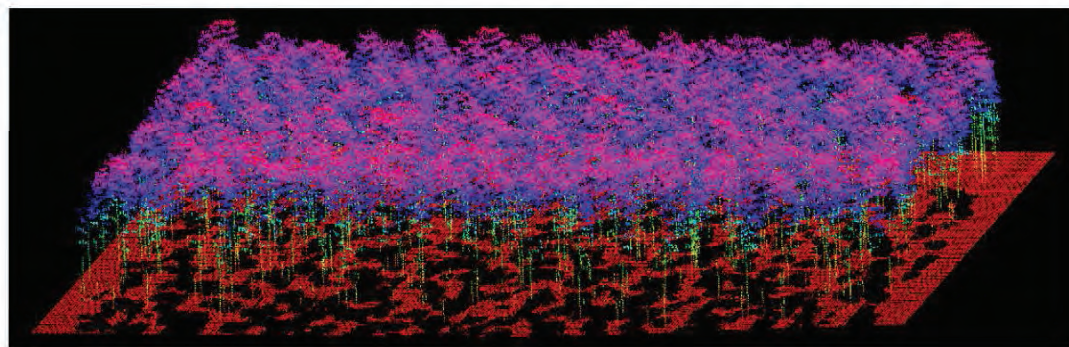
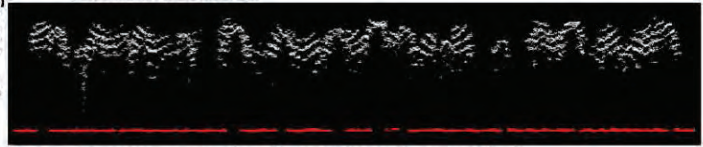
Waveform



Elevation



Classification



$\theta_L = 45^\circ$ at the center of swath

Height (z axis)

Cross-track direction (-y axis)